



**Phosphorus and its effects on the current  
efficiency in aluminium electrolysis**

Petre Manolescu

Thesis of 30 ECTS credits

**Master of Science in Mechanical Engineering**

January 2014

# **Phosphorus and its effects on the current efficiency in aluminium electrolysis**

Petre Manolescu

30 ECTS thesis submitted to the School of Science and Engineering  
at Reykjavík University in partial fulfillment  
of the requirements for the degree of  
**Master of Science in Mechanical Engineering.**

January 2014

Student:

---

Petre Manolescu

Supervisor(s):

---

Dr. Guðrún Arnbjörg Sævarsdóttir

Examiner:

---

Dr. Ari Jónasson

---

## Abstract

In the process of aluminium electrolysis impurities play an important role in lowering the current efficiency. Phosphorus is such an impurity which enters the electrolyte along with the alumina. It can have valence states from -3 to +5 and it can therefore take part in cyclic redox reactions. Phosphorus can be expelled with the anode gases, as elemental phosphorus or, attached to carbon dust [22]. However, due to the use of dry scrubbers it finds its way back to the electrolysis cell along with the secondary alumina.

Experiments were carried out in a laboratory cell at the Norwegian Institute of Science and Technology where different concentrations of  $\text{AlPO}_4$  were introduced in the melt. In order to notice the effects of phosphorus on the current efficiency a stable concentration of phosphorus was needed within the electrolyte for the duration of the experiments. The first step was to determine how much and if any phosphorus escapes the laboratory cell during the performance of the experiments. It was found that that in the short time the experiments were running there was little to none phosphorus escaping the melt. Further experimental work with different current densities as well as phosphorus concentrations showed a correlation between the initial amount of phosphorus and the current efficiency.

The present thesis establishes the theoretical background along with the experimental details.

---

## Acknowledgement

This work was done under the supervision of professor Dr. Guðrún Arnbjörg Sævarsdóttir, dean of the engineering department at the University of Reykjavík. I would like to thank her for her guidance and support over the last two and a half years. It has been a privilege to have her as my mentor.

This project was done in collaboration with Rauan Meirbekova as part of her doctoral research, sponsored by Alcoa. I would like to express my gratitude towards her for the experiments performed together.

I would like to thank Professor Dr. Geir Martin Haaberg, at the Institute for Materials Technology at NTNU, Trondheim, for his guidance during my stay there. It has been of great help to be able to turn to him when in doubt about certain aspects regarding the project.

Ove Darell and Henrik Gudbrandsen, researchers at Sintef have helped me a great deal with the practical part of this work, for which I am very grateful. I would like to thank Henrik Åsheim, Ph.D. student at NTNU, and Dr. Rebecca Jayne Thorne as well for their help with the laboratory work.

Finally, I would like to thank my parents for their moral and financial support as well as specialist support throughout the years of my education.

Petre Manolescu  
2014

# Contents

	Page
<b>1 List of symbols</b>	<b>5</b>
<b>2 Introduction</b>	<b>6</b>
2.1 History . . . . .	6
2.2 Process basics . . . . .	7
2.3 Current efficiency . . . . .	8
2.4 Purpose of the thesis . . . . .	8
<b>3 Theory</b>	<b>9</b>
3.1 Electric current . . . . .	9
3.2 Electrochemistry . . . . .	9
3.3 Decomposition potential . . . . .	10
3.4 Overpotential . . . . .	11
3.4.1 Concentration overpotential . . . . .	13
3.4.2 Diffusion overpotential . . . . .	15
<b>4 The Hall-Héroult process</b>	<b>18</b>
4.1 Process . . . . .	18
4.2 Bath chemistry . . . . .	20
4.3 Current Efficiency . . . . .	22
4.4 Impurities . . . . .	23
<b>5 Phosphorus</b>	<b>26</b>
5.1 General chemistry . . . . .	26
5.2 Impurity distribution in the aluminium electrolysis cell . . . . .	29
5.3 The effects of phosphorus in the aluminium cell . . . . .	31
5.4 Phosphorus circulation in the industrial process . . . . .	33
5.5 Electrochemistry of phosphorus . . . . .	34
<b>6 Experiments</b>	<b>37</b>
6.1 Purpose of the experiments . . . . .	37
6.2 Equipment setup . . . . .	38
6.3 Procedure . . . . .	40
6.4 Experimental cases I - Results and discussion . . . . .	43
6.5 Experimental cases II - Results and discussion . . . . .	45
6.6 Conclusions and further work . . . . .	47
<b>References</b>	<b>48</b>

# 1 List of symbols

Symbol	Units	Description
$a_i$	activity of species i	
A	Area	[m <sup>2</sup> ]
c	Concentration of species	[mol/m <sup>3</sup> ]
D	Diffusion coefficient	[m <sup>2</sup> /s]
<b>E</b>	Electric field	[V/m]
E	Decomposition potential	[V]
E°	Reversible potential	[V]
F	Faraday's constant	96487 C/mol
ΔG	Change in Gibbs energy	[J/mol]
I	Electric Current	[A]
j	Current density	[A/cm <sup>2</sup> ]
j <sub>0</sub>	Exchange current density	[A/cm <sup>2</sup> ]
K	Equilibrium constant	
k	Rate constant	[m/s]
M	Molar weight	[g/mol]
n	Number of electrons transfered	
Q	Coulomb	[C]
R	Resistance	[ω]
R	Gas constant	8.314 J/mol·K
r <sub>i</sub>	Radius of ion i	[m]
t	Time	[s]
T	Temperature	[K]
U	Cell voltage	[V]
V	Voltage	[V]
v	Velocity	[m/s]
z	Number of electrons transfered	
$\beta$	Symmetry parameter	
δ	Diffusion layer thickness	[m]
ν	Viscosity	[kg/s· m]
η	Overpotential	[V]

## 2 Introduction

### 2.1 History

Aluminium is the third most abundant element in the Earth's crust accounting for 8.3% by weight [11], with the first two elements being oxygen and silicon. Today aluminium is a widely used non-ferrous metal. Its applications have a very wide range from transportation to packaging, construction, electrical power lines, household items and more. However, its presence in everyday life is relatively new.



Figure 1: Alum [3]

Uses of aluminium date back to the ancient romans which used it in the form of alum (potassium aluminium sulfate) to stop bleeding [12]. Later on through the middle ages the production of alum increased to 1500 tonnes a year becoming a papal monopoly in Europe due to large deposits of alunite in papal states. However, the monopoly ceased when alum was discovered in abundance in north Yorkshire thus allowing the English to start their own production. As mentioned above alum was used to stop bleeding, but for colouring fabrics as well.

Due to its strong bond with oxygen the aluminium has been difficult to extract from its oxide until the second half of the nineteenth century. The first successful attempts to produce the metal came in 1809 from Sir Humphry Davy who isolated an impure form from alum. In 1855 France, H. Sainte-Claire Deville managed to reduce aluminium chloride with sodium. However the product was less than 95% pure and the cost for the process was too high[13]. Other trials were made in 1825 by Hans Christian Oersted in Denmark who obtained an impure form by heating aluminium chloride with potassium metal. Fredrich Wöhler from Germany used sodium instead of potassium thus managing to obtain a pure sample[12].

The breakthrough came in 1886 when two young students were able to extract aluminium from molten aluminium salts using an electric current. The process was developed independently and almost simultaneously by Charles M. Hall in the United States of America and Paul Héroult in France. After filing for a patent on the process it, was decided that Hall would have the rights in America and Héroult in Europe.

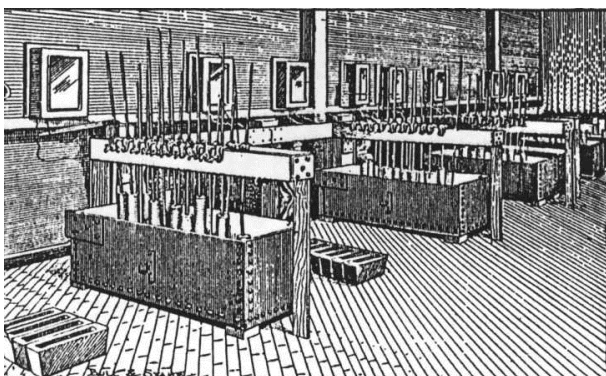


Figure 2: Early Hall Cell at the Pittsburg Reduction Company [5]

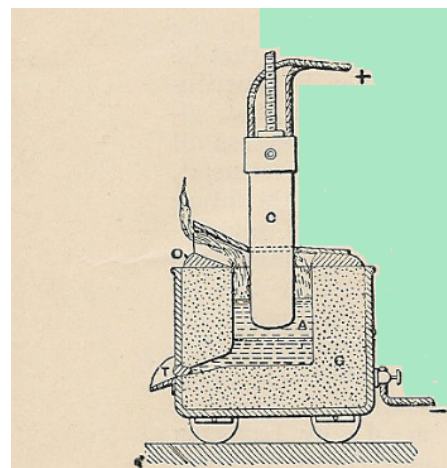


Figure 3: Section of the early Héroult cell [4]

## 2.2 Process basics

Alumina is the main source of aluminium. The oxide is extracted from bauxite through the Bayer process. Aqueous solutions are not suitable as electrolytes since hydrogen is electrochemically nobler than aluminium and would therefore not dissolve the alumina. So far, the only electrolyte available is cryolite ( $\text{Na}_3\text{AlF}_6$ ). Originally, natural cryolite was used but today the industry uses artificial cryolite since natural occurrence is hard to find and the modern Hall-Heroult process actually produces bath rather than consumes it. Fluorides additives such as  $\text{AlF}_3$ ,  $\text{CaF}_2$ ,  $\text{LiF}$  are mixed with the electrolyte in order to improve different parameters such as lower operating temperature or higher electrical conductivity. Cryolite melts at  $1012^\circ\text{C}$  but cells operate at a temperature between  $940$  and  $970^\circ\text{C}$ . Usual bath compositions are  $6 - 13 \text{ wt}\% \text{AlF}_3$ ,  $4 - 6 \text{ wt}\% \text{CaF}_2$ ,  $2 - 4 \text{ wt}\% \text{Al}_2\text{O}_3$ [31]. Lowering the melting point of cryolite reduces the alumina solubility however.

By applying a dc current through the electrolyte, molten aluminium pools at the cathode. The electrolytic cell consists of a steel shell lined with carbon which serves as the cathode. Molten cryolite is highly corrosive so in order to keep the cell from damage a side ledge of frozen cryolite is formed on the inside of the carbon cathode by careful management of heat transfer through the cell walls.

The anodes are consumable and they are made of carbon. The preferred type are prebaked, made at specialized anode plants and are a mixture of pitch and petroleum coke. The second type, nowadays rare, are Söderberg anodes which are continuous baking. The prebaked anodes need changing on a regular basis since the carbon reacts with the oxygen from the alumina forming carbon dioxide. A mixture of alumina and frozen bath makes up the crust used on top of the cell in order to protect the anodes from air burn and prevent moisture and other impurities from entering the bath. A crust breaker is used to break through it when feeding needs to be done.

A schematic drawing of an aluminium cell is shown in the figure below:

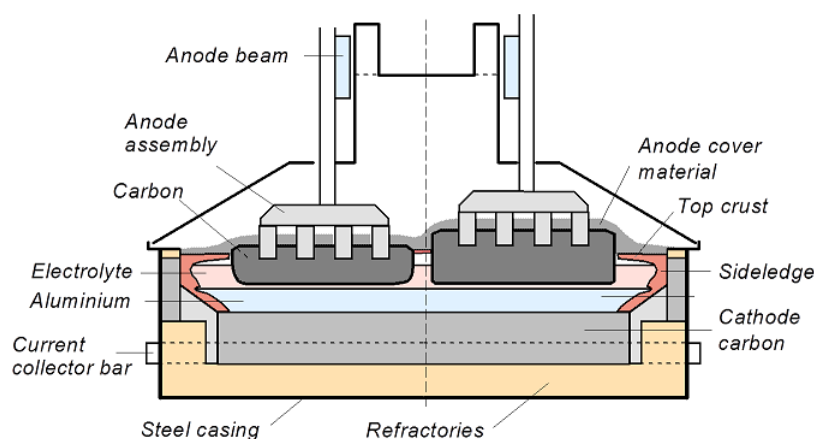
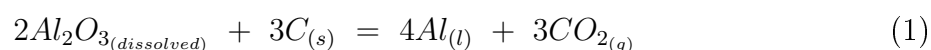


Figure 4: Schematic drawing of an aluminium cell [10]

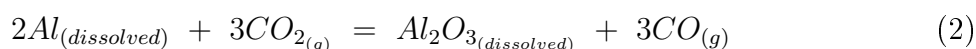
The overall chemical reaction can be written as:



## 2.3 Current efficiency

One of the most important parameters in aluminium production is the current efficiency. It is a measure of how much of the current passed through the cell actually produces metal. There are several methods that can be used to measure it but none is in real time. The most common way is to take the ratio of the weight between the produced metal and the theoretical amount that should be obtained according to Faraday's first law. Technological advancement and better understanding of the process have allowed modern cells to reach current efficiencies of close to or even above 95% [14].

Since aluminium is slightly soluble in molten cryolite some of the metal will appear as dissolved in the electrolyte. When it comes in contact with carbon dioxide it can react forming dissolved alumina and carbon monoxide. This mechanism is known as the back reaction and it is the main source of current efficiency losses. The reaction can be written according to:



Other important factors that influence the current efficiency of the electrolysis cell are impurities in the cryolite melt, operating temperature and cell design. The impurities can be metal oxides, non-metal oxides, sulphurous compounds and water. They enter the electrolyte as part of the raw materials, namely alumina. Others are found in the carbon that makes up the anodes, in the compounds that form the electrolyte, tools used in the pot room and moisture absorbed by the materials. Impurities have a detrimental factor towards current efficiency since they are reduced and/or oxidized within the bath. Some of them are expelled as anode gases but, others can deposit in the metal produced, diminishing its quality.

Another important parameter is the energy consumption. This measure of cell performance includes both cell voltage and current efficiency. In today's cells the value is about 13 kWh/kg Al produced. However, the theoretical energy consumption is 6.34 kWh/kg Al. Therefore, the total energy efficiency is usually below 50%. The remaining percentage is lost as heat to the surroundings.

## 2.4 Purpose of the thesis

As mentioned above, impurities in the electrolyte affect the current efficiency. Polyvalent impurity species take place in cyclic redox reactions thus consuming energy [23]. The impurity of interest in this thesis is phosphorus which enters the bath with the alumina and can have valence states from -3 to +5 [22]. The anode gases are recycled and impurities accumulate in the secondary alumina, phosphorus being one of them. As a result phosphorus enters the bath once again and the cycle repeats.

Experiments were made in a laboratory cell at the Sintef laboratory within the Norwegian University of Science and Technology. According to Augood [32] phosphorus forms volatile compounds and escapes the cell with the anode gases. Therefore, the first step was to determine how much, if any, phosphorus escaped from the cell during the experiments. This lays the ground work for further investigations of the effects of phosphorus to the current efficiency where different concentrations as well as current densities are used.

## 3 Theory

### 3.1 Electric current

An electric current consists of a stream of flowing electric charges. Within electric circuits of metallic nature the current is transported by electrons, therefore named electronic conduction. The electric current is defined as the amount of charge that passes in a given timeframe. The SI unit is an Ampere, A.

$$I = \frac{Q}{t} \quad (3)$$

An electric current is induced in a circuit by applying a potential difference within it. The ability to conduct electric current varies according to the material of the circuit. Therefore the current can be calculated from Ohm's law which ties together the potential difference and the resistance of the circuit.

$$I = \frac{V}{R} \text{ or } V = IR \quad (4)$$

where V is the voltage measured in Volts and R is the resistance measured in Ohms.

### 3.2 Electrochemistry

An electric field can be induced in an electrolyte by applying a dc potential difference between two electrodes. The electrodes are electronic conductors containing free electrons such as metals, semiconductors or carbon in solid or liquid state. This will result in motion of the ions within the electrolyte, which will move with the electric field or against it depending on whether they are positive or negative ions. Charge transfer will take place and therefore electric current begins to flow.

A simple electrolytic cell is shown schematically in the figure below:

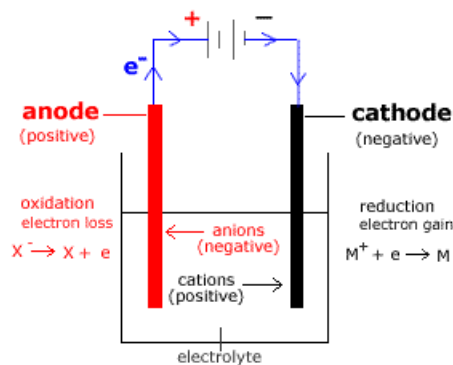


Figure 5: Schematic drawing of an electrolysis cell [19]

The electrodes are charged negatively (cathode) and positively (anode). Since charges of opposite signs will attract, the positive ions (cations) will move towards the cathode and the negative ions (anions) will move towards the anode. The loss of electrons takes place at the anode and is referred to as the oxidation reaction. The gaining of electrons takes place at the cathode and is called reduction reaction.

The conductance of the electrolyte can be shown to depend on the nature of the ions dissolved, their concentration, and the viscosity of the molten salt which is a function of the temperature. The electric field depends on the area of the electrodes and the distance between them. The current that passes through area A can be expressed as:

$$i = i^+ + i^- = \frac{dQ^+}{dt} + \frac{dQ^-}{dt} = e_0(n^+z^+v_{max}^+ + n^-z^-v_{max}^-)$$

The mobility (denoted "u") of the ions is defined as the ratio between the maximum velocity and the strength of the electric field and the current per unit area can be expressed as:

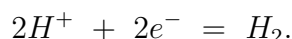
$$i = Ae_0(n^+z^+u^+ + n^-z^-u^-) \cdot |\mathbf{E}|$$

The magnitude of the electric field can be expressed as the ratio between the potential difference between the electrodes ( $\Delta V$ ) and the distance between them (l). Another way of writing the electric current is as the product between conductance (L) and the potential difference  $i = L\Delta V$  where the conductance (L) is given by  $(A/l)e_0(n^+z^+u^+ + n^-z^-u^-)$ .

### 3.3 Decomposition potential

In order to start the electrolysis process the applied potential has to be greater than the reversible potential of the reaction. The reversible potential of a cell is the measured voltage when no current is flowing through it and is therefore at equilibrium, denoted  $E^\circ$ . Since there are always two reactions taking place in an electrolytic cell the voltage between the electrodes can be considered to be the sum of two half-cell voltages. It is, however, impossible to determine the absolute value of the voltage of a single half-cell [14]. A relative scale is used to overcome this problem. Due to the abundant information existing, aqueous solutions are used as an example to illustrate the theory behind the standard potential. The reference electrode is the standard hydrogen electrode (SHE) and its assigned voltage is zero.

The reaction taking place is



All other half-cell potentials are expressed relative to SHE. Some standard electrode potentials are shown in the table below.

Cathode(Reduction)half-reaction	Standard Potential $E^\circ$ (volts)
$K_{(aq)}^+ + e^- \Rightarrow K_{(s)}$	-2.92
$Na_{(aq)}^+ + e^- \Rightarrow Na_{(s)}$	-2.71
$Al_{(aq)}^{3+} + 3e^- \Rightarrow Al_{(s)}$	-1.66
$2H_2O_{(l)} + 2e^- \Rightarrow H_{2(g)} + 2OH_{(aq)}^-$	-0.83
$Fe_{(aq)}^{2+} + 2e^- \Rightarrow Fe_{(s)}$	-0.41
$Fe_{(aq)}^{3+} + 3e^- \Rightarrow Fe_{(s)}$	-0.04
$2H_{(aq)}^+ + 2e^- \Rightarrow H_{2(g)}$	0
$Cu_{(aq)}^{2+} + e^- \Rightarrow Cu_{(aq)}^+$	0.16
$AgCl_{(s)} + e^- \Rightarrow Ag_{(s)} + Cl_{(aq)}^-$	0.22
$Fe_{(aq)}^{3+} + e^- \Rightarrow Fe_{(aq)}^{2+}$	0.77
$O_{2(g)} + 4H_{(aq)}^+ + 4e^- \Rightarrow 2H_2O_{(l)}$	1.23

Table 1: Standard electrode potentials in Aqueous Solution at 298K[33]

Spontaneous reactions are the ones which have a positive standard electrode potential. When the standard electrode potential is negative energy needs to be supplied in order to start the reaction. The decomposition potential can be calculated from the Nernst equation which takes into account the reversible potential, the activities of the species involved and the temperature at which the reaction is taking place. The equation is given below:

$$E = E^\circ - \frac{RT}{nF} \ln(K_e) \quad (5)$$

where R is the gas constant, T the temperature in Kelvin, n the number of electrons transferred in the reaction, F Faraday's constant.  $K_e$  is the equilibrium constant determined by the ratio of the activities of the products and reactants, which, for a general reaction, is found according to:

$$bB + cC = mM + nN \Rightarrow K_e = \frac{a_M^m \cdot a_N^n}{a_B^b \cdot a_C^c}. \quad (6)$$

### 3.4 Overpotential

A boundary layer forms between the electrode and electrolyte surface. The simplest model is the Helmholtz model which is shown in the figure below.

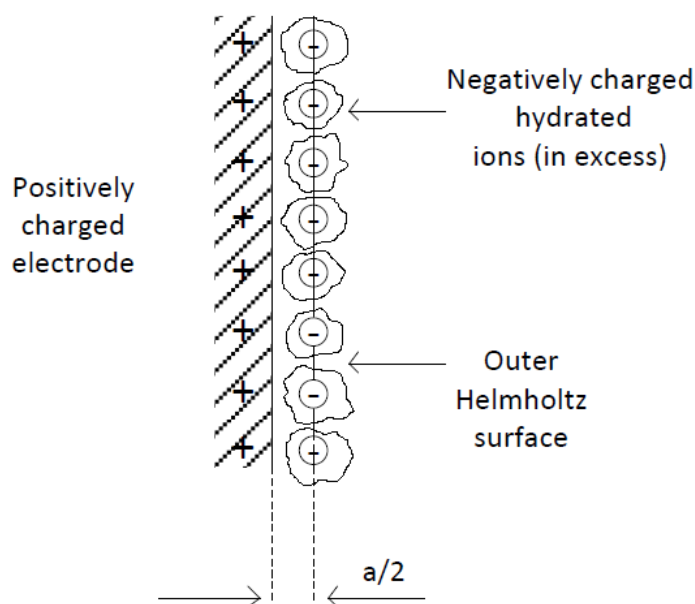


Figure 6: Helmholtz double layer for an aqueous solution of width  $a/2$  where,  $a$  is the diameter of the solvated counter ion. [9]

A phase boundary will form between the electrode and the solution. Charges opposite to that of the electrode approach the electrode from the electrolyte. When they are as close as possible there will be two parallel lines of charge of opposite signs which will behave as a capacitor. When the currents are low the limiting factor is the rate of electron transfer across the boundary layer between the electrode and the ionic solution. The rate of change of electrode potential with current is termed electron transfer overpotential, which depends on the species involved in the reaction[9]. In other

words, the reaction rate is too slow at the applied voltage so an extra amount of energy needs to be supplied in order for the reaction to take place at its appropriate rate[14].

According to [9] the concept of overpotential is defined as the deviation of the anodic or cathodic electrode potential from the equilibrium value. Alternatively, the overpotential is the potential that must be added to the reversible potential in order to run a reaction at a certain rate.

$$\eta = E - E_{eq}$$

In order to illustrate this important factor clearly the simplified form of the system  $H_2|Cl_2$  is taken as an example. The variation of cell voltage with current is shown schematically when the cell is running as a galvanic cell versus an electrolysis cell with HCl as electrolyte. It must be mentioned that the voltage versus current behaviour is normally exponential and not linear as depicted below for simplicity.

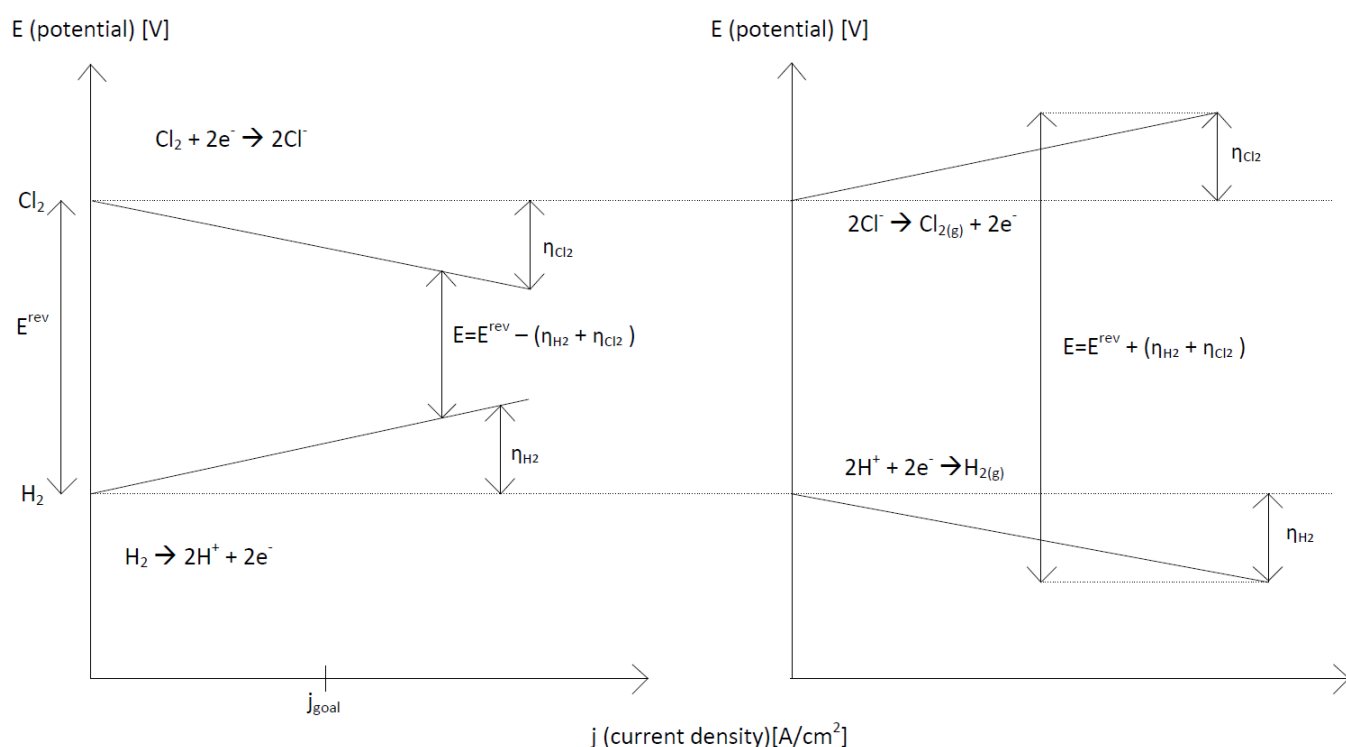


Figure 7: Variation of cell voltage with current between a galvanic cell and electrolysis cell[9]

The types of overpotentials that need to be considered when calculating the total cell voltage needed to perform the electrolysis are the activation overpotential, diffusion overpotential and the reaction (concentration) overpotential. Diffusion overpotential appears at high current densities when the limiting factor is the transport of reactants from the solution to the electrode surface. The reaction overpotential takes place when the chemical reactions cannot keep pace with the electron transfer step[9].

The activation overpotential gives a measure of the activation energy that needs to be overcome in order for electron transfer to occur. The relationship between the activation overpotential and current density is given by the Butler-Volmer equation:

$$j = j_a - j_c = j_0 \left[ \exp \left( \frac{\beta n F \eta}{RT} \right) - \exp \left( - \frac{(1 - \beta) n F \eta}{RT} \right) \right] \quad (7)$$

where  $j_a$  and  $j_c$  are the anodic and cathodic current densities and  $j_0$  is the exchange current density which is a measure of the rate of electron transfer at equilibrium given by:

$$j_0 = n F k^\circ a_{ox}^{\beta \frac{z}{n}} a_R^{(1 - \beta \frac{z}{n})} \quad (8)$$

where  $a_{ox}$  and  $a_R$  are the activities of the oxidized and reduced species while  $k^\circ$  is standard rate constant,  $\beta$  is the symmetry parameter,  $z$  is the number of electrons transferred in the rate determining step and  $n$  are the number of electrons transferred in the overall reaction. The Butler-Volmer relationship is the limiting factor when the main reaction is charge transfer controlled. However in aluminium production the reaction is mass transfer controlled.

### 3.4.1 Concentration overpotential

The concentration overpotential arises when the species involved in the reaction cannot be transported fast enough between the electrode surface and the bulk of the electrolyte. As a result the species involved will have different concentrations at the electrode surface ( $c^s$ ) and the bulk ( $c^0$ ). Usually  $c^s < c^0$ . In order to adjust the rate of transport to an even flow, an overpotential must be applied, namely concentration overpotential. The total overpotential can therefore be written as the sum between the charge-transfer overpotential( $\eta_{el}$ ) and the concentration overpotential( $\eta_{co}$ ):

$$\eta_{total} = \eta_{el} + \eta_{co} \quad (9)$$

When dealing with high anodic overpotentials it can be assumed that the current density is  $j \approx j_a$  therefore:

$$j_a = n F c_{Red}^s k_0^+ \exp \left( \frac{(1 - \beta) F E^{rev}}{RT} + \frac{(1 - \beta) F \eta}{RT} \right) \quad (10)$$

When  $c_{Red}^s = c_{Red}^0$  the exchange current density is:

$$j = j_0 \frac{c_{Red}^s}{c_{Red}^0} \exp \left( \frac{(1 - \beta) F \eta}{RT} \right) \quad (11)$$

Rearranging and isolating  $\eta$  gives:

$$\eta = \frac{RT}{(1 - \beta) F} \ln \left( \frac{j}{j_0} + \frac{c_{Red}^0}{c_{Red}^s} \right) \quad (12)$$

The equation above is an expression of the total overpotential given by (9) therefore the anodic concentration overpotential can be written as:

$$\eta_{co} = \frac{RT}{(1 - \beta) F} \ln \left( \frac{c_{Red}^0}{c_{Red}^s} \right) \quad (13)$$

For the cathodic process a similar equation can be obtained:

$$\eta_{co,c} = - \frac{RT}{\beta F} \ln \left( \frac{c_{ox}^0}{c_{ox}^s} \right) \quad (14)$$

In the context of aluminium electrolysis a detailed study of the available literature was done by Thonstad et al. [1]. The cathodic overvoltage is mass transfer controlled therefore it is a concentration overpotential. The cathodic overvoltage is of the order 50-100 mV at normal cathodic current densities ( $0.4 - 0.7 \text{ A/cm}^2$ ) and normal temperatures ( $970 - 1010^\circ\text{C}$ ). The cell design and the convection pattern of the cell influence the magnitude of the overvoltage so by stirring the melt the overvoltage could be reduced. The ratio of the diffusion coefficient and the thickness of the boundary layer gives the mass transfer coefficient of the reactant. This is the determining factor for the concentration overpotential. Assuming there is no charge transfer overvoltage and therefore chemical equilibrium at the interface, the effect of the concentration gradient in the boundary layer can be expressed. By taking the general equation (14) and adjusting it to the context of aluminium electrolysis the following is obtained:

$$\eta_c = -\frac{RT}{3F} \left[ \ln \left( \frac{a_{\text{AlF}_3}^*}{a_{\text{AlF}_3}} \right) \left( \frac{a_{\text{NaF}}}{a_{\text{NaF}}^*} \right)^3 \right] \quad (15)$$

or since the sodium ion is the carrier of current it can be written as:

$$\eta_c = \frac{RT}{F} \ln \left( \frac{a_{\text{Na}}}{a_{\text{Na}}^*} \right) \quad (16)$$

where the  $a^*$  represents the activities of the given species at the metal/electrolyte interface while the others are the activities in the bulk. The mass transfer in the boundary layer is shown schematically in the figure below. The distance from the electrode surface is represented by  $\delta$  which is, in other words, the diffusion layer thickness.

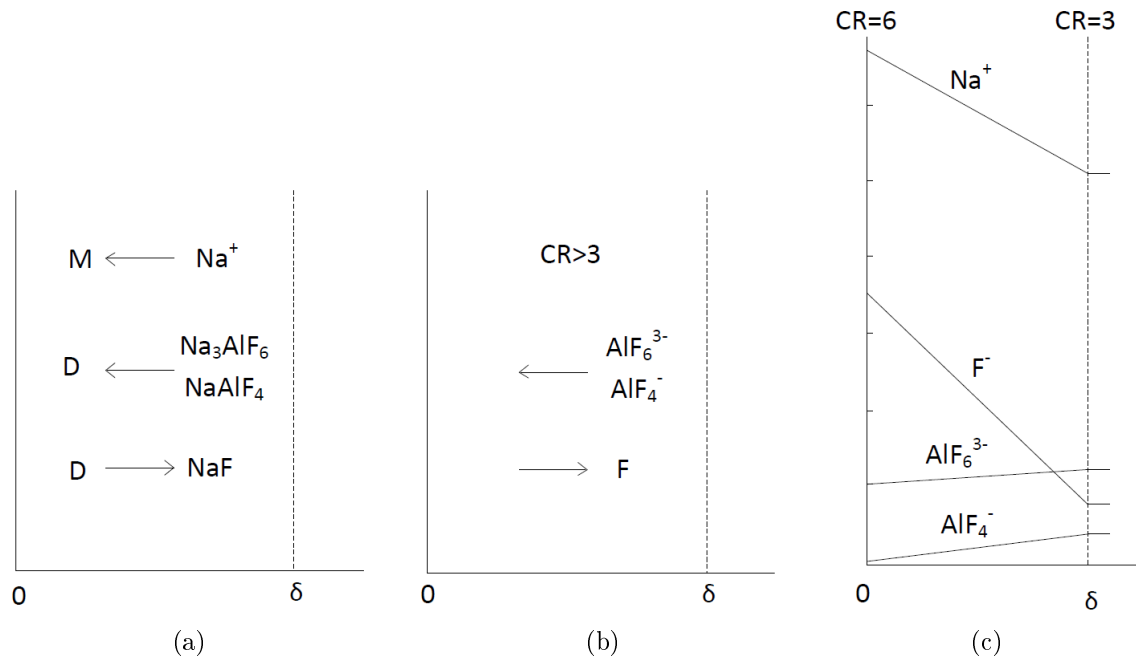


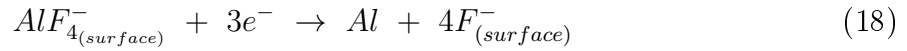
Figure 8: a) Formal treatment. b) Net ionic transport. c) Cathodic overvoltage. [1]

The mass transfer takes place through migration of sodium ions which transport the current, while aluminium is being discharged and  $\text{NaF}$  diffuses back. The net ionic transport is given in figure 8(b). The only moving species are the aluminium complexes and

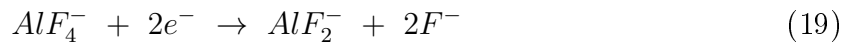
the fluor ions. The  $F^-$  ions carry negative charge and move away from the cathode to preserve electro-neutrality as aluminium is discharged. The process can be described by the following reactions: Diffusion towards the electrode:



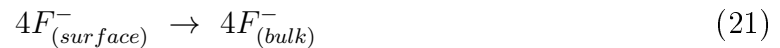
A two-step reduction charge transfer reaction: Overall reaction



Two-step reduction:



Counter-current transport of charge:



Similar reactions can be derived for the  $AlF_6^-$  or oxyfluorides as the electroactive ions. The cathodic overvoltage is shown in figure 8(c). Increasing the current density results in increasing the overpotential and the concentration of the sodium ions. By increasing convection the overpotential decreases and the concentration of the sodium ions as well. However, in this case the current efficiency will decrease as well.

### 3.4.2 Diffusion overpotential

The concentration profile of a metal ion is shown in the figure 9 as a function of the distance from the electrode surface. Initially, when no current runs through the concentration is a flat line marked bulk concentration on the graph. As current is passed through the system the surface concentration decreases to a value close to zero in this example. The Nernst diffusion layer thickness is the amount by which the concentration profile formed extends into the solution near the electrode surface. The layer thickness is denoted by  $\delta_N$  and its magnitude is determined by the intersection of the tangent to the concentration profile near the electrode surface with the bulk concentration line. Another important factor is that it is time dependent and increases with the total charge passed through the system until it reaches equilibrium. The attainment of steady state takes longer when the solution is still rather than when it is stirred.

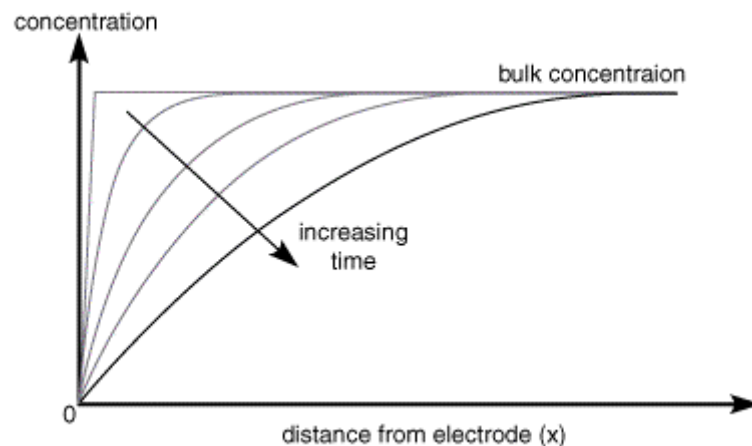


Figure 9: Development of concentration with time after onset of current flow [26]

At high overpotentials the current density is determined by the rate of diffusion. Fick's first law states that

$$J = -D\nabla c \quad (22)$$

where J is the mass flux, D the diffusion coefficient and c is concentration. By combining it with Faraday's law  $j=nFJ$  the following expression is obtained:

$$j = nFD \left( \frac{\delta c}{\delta x} \right)_{x=0} = nFD \frac{c^0 - c^s}{\delta_N} \quad (23)$$

As  $c^s \rightarrow 0$  the current density tends to a limiting value becoming:

$$j_{lim} = nFD \frac{c^0}{\delta_N} \quad (24)$$

The Nernst equation relates the concentration of the metal ion to the standard electrode potential, namely:

$$E = E^0 + \frac{RT}{zF} \ln(c^0) \quad (25)$$

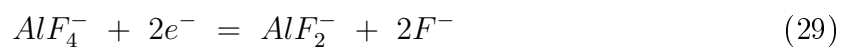
When the electrochemical rate is extremely fast the overpotential will have the form:

$$\eta_d = \frac{RT}{zF} \ln \left( \frac{c^s}{c^0} \right) \quad (26)$$

By taking the ratio of equation (23) to (24) an expression for the diffusion overpotential can be found:

$$\frac{j}{j_{lim}} = 1 - \frac{c^s}{c^0} = 1 - \exp \left( \frac{zF\eta_d}{RT} \right) \Rightarrow \eta_d = \frac{RT}{zF} \ln \left( 1 - \frac{j}{j_{lim}} \right) \quad (27)$$

The charge transfer reaction in aluminium electrolysis is fast giving a charge transfer overvoltage of only a few millivolts. An overview of the work performed in this field is given by Thonstad et al. [1]. The cathodic charge transfer reaction is described as a chemical step followed by two charge transfer steps, with a likely scheme being:



The last reaction is the faster charge transfer step with an exchange current density higher than 20A/cm<sup>2</sup>. The exchange current density of the first charge transfer step varies from around 8 to 1 A/cm<sup>2</sup> with increasing alumina content. The rate constant for the chemical reaction preceeding the charge transfer steps was found to be in the range of 2000 to 8000 s<sup>-1</sup> thus being a rather fast reaction.

All of these overpotentials influence the total cell voltage in aluminium electrowinning. Alumina decomposes according to the reaction



In equation 31 the carbon, aluminium and carbon dioxide can be considered to be in their standard states since they are nearly pure phases. Alumina however, can only be considered in its standard state only at saturation. Therefore its activity has to be taken

into consideration and the decomposition potential is given by the Nernst equation 5. For compounds in their standard state the decomposition potential is given by the equation:

$$E^{\circ} = \frac{-\Delta G}{nF} \quad (32)$$

According to [2] the decomposition potential of alumina is calculated to be -1.223 V. Therefore the cell voltage must be higher than the decomposition potential of alumina. The overall cell voltage in aluminium electrolysis can be written as[14]:

$$U = |E^{rev}| + |\eta_{cc}| + |\eta_{aa}| + |\eta_{ac}| + U_R + U_E \quad (33)$$

where U is the cell voltage,  $E^{rev}$  is the reversible potential,  $\eta_{cc}$  is the concentration overvoltage at the cathode,  $\eta_{aa}$  is the reaction overvoltage at the anode,  $\eta_{ac}$  is the concentration overvoltage at the anode,  $U_R$  is the ohmic voltage drop in the electrolyte and  $U_E$  is the sum of cathode, anode and other external voltage drops.

## 4 The Hall-Héroult process

### 4.1 Process

The production of aluminium involves the dissolution of alumina in molten cryolite which results in liquid aluminium deposition at the cathode. Since its invention many technological advances have been made due to better understanding of the process, but the initial principle still remains at its core. The main reaction can be written as:



The electrolysis takes place in carbon-lined steel tanks with carbon anodes. The true cathode is the molten aluminium that accumulates at the bottom due to higher density than the electrolyte. Molten cryolite ( $Na_3AlF_6$ ) is highly corrosive and thus the cell is lined with frozen cryolite.

Alumina,  $Al_2O_3$ , is the main raw material which is derived from bauxite through the Bayer process. The alumina is fed from the top of the cell, after breaking the crust formed from anode cover material. The cell operates at a voltage of about 4.2 V and currents as high as 350kA and up to 700kA in China.

The current is passed through the cell along carbon anodes that can be prebaked or continuous self-baking Söderberg type. The former is the more prevalent version due to higher current efficiency and anode quality, therefore giving a higher production output. They are between 18 and 32 for each cell. Since carbon is consumed during the reaction the anodes need to be changed every 22-26 days or so. Steel collector bars attached to the carbon cathode allow the current to pass through to the next cell. The cells are connected in series forming a closed loop so as to minimize the electromagnetic field generated by the high current.



Figure 10: An aluminium potline [16]

The strong negative deposition potential of aluminium makes the electrolysis in aqueous solution impossible. Furthermore the aluminium ion has the tendency to be readily hydrolyzed [9]. Cryolite is a salt containing sodium, aluminium and fluor ( $Na_3AlF_6$ ) which can dissolve alumina. Although  $Al_2O_3$  has a melting point at about 2050°C it dissolves in the molten cryolite at around 950°C. In order to lower the operating temperature and increase the current efficiency other compounds can be found in the electrolyte such as calcium fluoride, aluminium fluoride and in some cases lithium fluoride.

In the industry alumina serves more roles than just as feeding material. It is one of the main components in anode cover material that protects it from heat and vapour losses, moisture from air entering the cell and avoid air-burn of the anodes. Another role is the use of alumina in the dry scrubbers. The gas from the process is fed in the scrubbers and alumina is used to absorb the hydrogen fluoride gas and other vapours. This alumina will have a high content of fluoride and is fed back into the bath as secondary alumina. Earlier systems were open and did not have dry scrubbers thus expelling the anode gasses straight into the atmosphere. The dry scrubbers have therefore the role of protecting the environment from the anode gasses and recycling the fluoride.

Current efficiency is one of the most important parameters in determining the performance of a cell. The easiest and most reliable form of measurement is by taking the ratio of the tapped metal versus the theoretical production at a given current magnitude within a certain amount of time. This ratio is never 100% due to impurities in the electrolyte, back reaction between dissolved aluminium in the bath and carbon dioxide, metal shorting at the anode, physical losses and metal losses in the cell lining [1].

As mentioned above there are two types of cells used in the industry. The first one uses prebaked anodes that are consumed and changed every three weeks or so and the second one involves self baking anodes. The prebake type is the most common due to higher anode purity and easier sealing which makes it more environmental friendly. It provides better current efficiency as well. The anodes are produced in dedicated anode plants. In some cases the anode plant and the aluminium smelting plant are close to each other like for example the Hydro plant in Ardal, Norway. The anodes contain 55 – 65% petroleum coke, 15 – 30% recycled butts and about 15% pitch. The paste is then mixed and calcined at 1250° in baking furnaces. The usual size of the anodes is 70cm wide x 125cm long x 50 cm high[15].

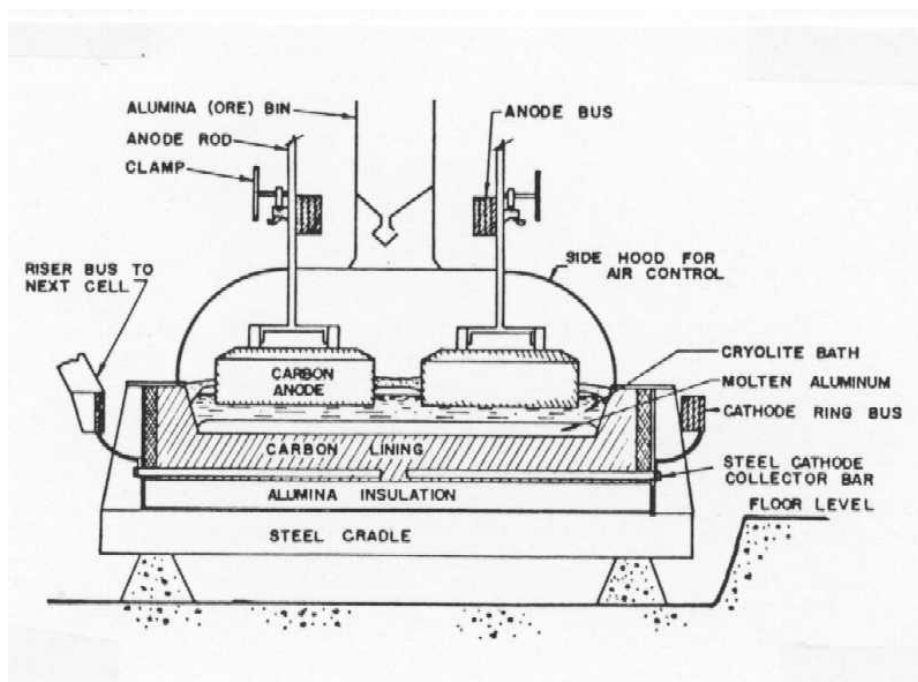


Figure 11: Modern cell with prebake anodes [27]

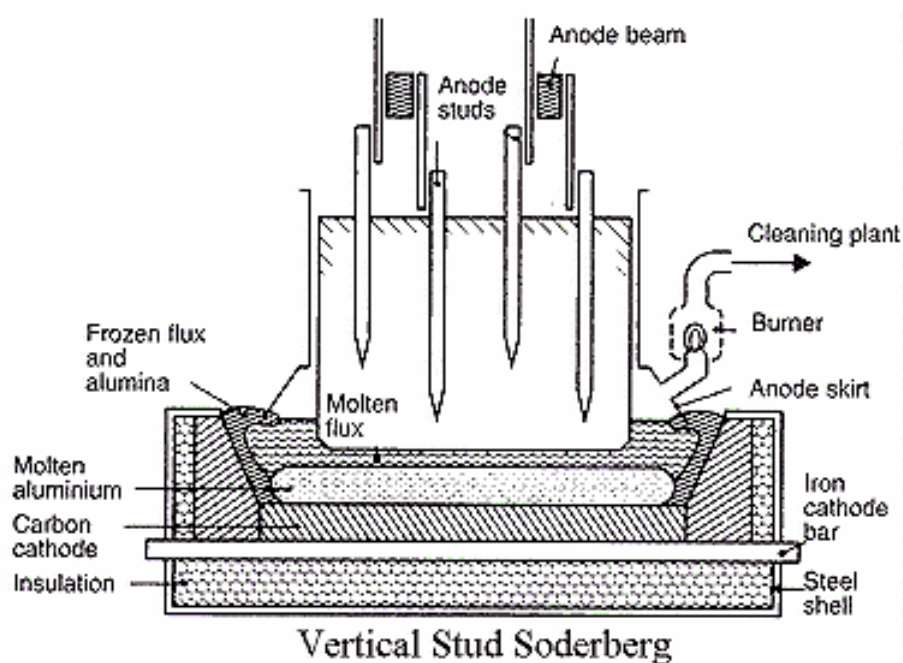


Figure 12: A Søderberg cell [28]

The second type of cell has a continuously baking anode of the Søderberg type. Anode material in the form of briquettes is loaded on the top of the electrode shell. These are a blend of petroleum coke and pitch. The temperature increases along the length of the anode case and as the briquettes go down they melt and then bake into a solid anode. The electrical contact is made by steel pins that can be introduced vertically or horizontally in the anode. Since these cells have one anode its surface area is much larger than the prebaked anode, therefore imposing a higher resistivity through the electrolyte. Other drawbacks are environmental issues associated with its operation. The higher resistivity translates into the loss of current efficiency therefore giving the Søderberg cells a lower value than the prebake cells. These issues and the development of better prebake anode production methods have contributed to the declining use of the Søderberg cells.

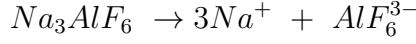
## 4.2 Bath chemistry

The main component of the aluminium bath is cryolite ( $\text{Na}_3\text{AlF}_6$ ). However additions are made to the cryolite in order to adjust its melting point as well as influencing the current efficiency. The usual additives are aluminium fluoride and calcium fluoride. A concentration of 3 to 10% of  $\text{CaF}_2$  is present at all times in the electrolyte[2]. Calcium oxide is one of the main impurities found in alumina which is fed into the bath. It reacts with the excess aluminium fluoride forming calcium fluoride and reaches a steady state concentration in the electrolyte. The stability of the concentration is a result of the balance between the rate of addition of  $\text{CaO}$  and the loss of calcium through anode gases.

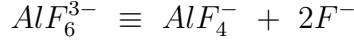
A measurement for the excess aluminium fluoride in the bath is the CR ratio which is the molar ratio between sodium fluoride and aluminium fluoride. In today's industrial process the ratio is between 2 and 3 [1]. One factor of great importance to the current efficiency is the presence of dissolved metal in the electrolyte. Addition of  $\text{AlF}_3$  to the cryolite melt reduces the solubility of metal in the bath. In the industry, typical values of

the solubility of aluminium in the melt are of the order 0.03 to 0.06 wt%Al[1]. Another effect of  $AlF_3$  is that it lowers the melting temperature of the electrolyte.

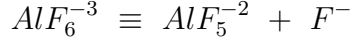
In the electrolyte the main current carriers are the  $Na^+$  ions. The cryolite melt is ionized according to



The hexafluoroaluminate ions dissociate further, mainly according to the reaction:



Some of it dissociates in the form of:



The degree of  $AlF_6^{3-}$  dissociation varies with the CR ratio[2]:

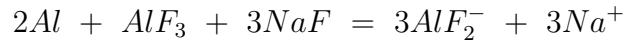
$NaF/AlF_3$ Molar Ratio	$AlF_6^{3-}$ Dissociation
3	25%
2	55%
1	100%

Table 2: The dissociation of hexafluoroaluminate ions

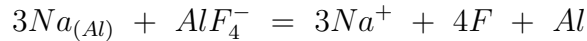
The concentration of dissolved sodium in the melt is higher at the aluminium-electrolyte interface due to the equilibrium:



Experiments carried out by Ødegård et al. [18] have shown that sodium dissolves in the melt as free Na while aluminium appears mostly as monovalent species  $AlF_2^-$ . Consequently the dissolution reaction was proposed as:

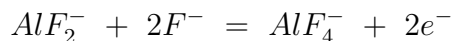


The current is conducted through the electrolyte by the sodium ions. The applied potential results in higher concentration of sodium ions at the aluminium-electrolyte interface compared to the concentration in the bulk. The following reaction at equipotential deposition equilibrates sodium with aluminium and cryolite. It is related to the concentration of  $Na^+$  ions in the bath near the cathode surface and would fix the sodium content in the aluminium-sodium alloy [17].



The presence of excess sodium at the aluminium-bath interface induces a counter-voltage that is called polarization. Electromagnetic stirring reduces the cathodic polarization in most industrial cells as compared to laboratory cells. The cathodic over-voltage increases with low CR ratio (high  $AlF_3$ ) and increased cathodic current density.

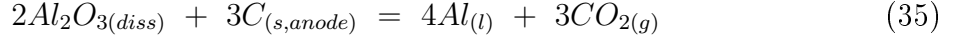
Another issue worth considering is the anodic oxidation of dissolved metal in the electrolyte. High values of the diffusion coefficient have been reported which led to a suggestion of an electron jump mechanism expressed by:



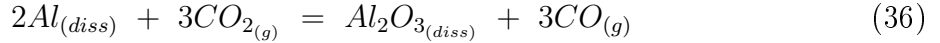
### 4.3 Current Efficiency

In the aluminium industry the current efficiency is a measurement of the operational performance of a cell. In other words it is a measure of how efficiently the current passed through the cell is used to reduce alumina to aluminium. In modern smelters the current efficiency can be as high as 96%[1].

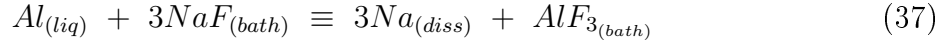
The main electrochemical reaction that produces aluminium can be written as:



The major loss in current efficiency is due to the back reaction of dissolved aluminium in the bath with carbon dioxide gas[2]:

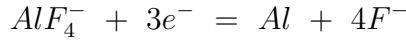


Another reaction that contributes to the loss of current efficiency is[2]:

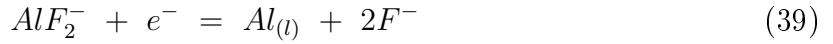
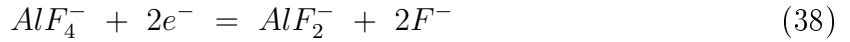


A more modern approach at setting up the losses is[1]:

Cathodic reaction:



This can further be divided in:



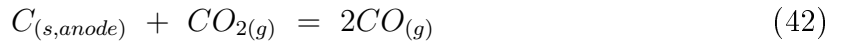
with the main side reaction being:



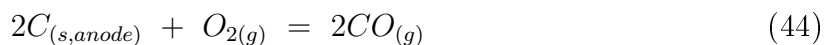
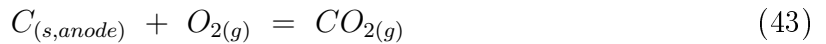
Even though the Pearson-Waddington equation gives an instantaneous measure of the current efficiency, it relies on the assumptions that  $CO_{2(g)}$  is the only anode product and that all of the  $CO_{(g)}$  is produced by the back reaction shown in equation 36. This technique essentially measures the ratio between the carbon dioxide and carbon monoxide gases and is calculated according to:

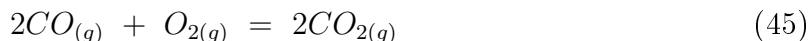
$$CE(\%) = 100\% - 0.5[\%CO_{(g)}] = 50\% + 0.5[\%CO_{2(g)}] \quad (41)$$

The reason for its inaccuracy are several possible reactions that take place within the cell affecting the  $CO_{2(g)}/CO_{(g)}$  ratio in the anode gas. The most important ones are the Boudouard reaction:

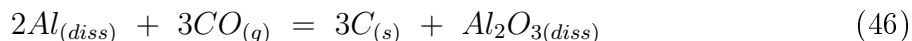


Other reactions may occur between air and carbon or carbon monoxide:





Additionally solid carbon can be formed by the reaction of dissolved aluminium with carbon monoxide gas:



There are however, other factors that influence the current efficiency of a cell. When the cathode becomes exposed due to lack of solid cryolite cover the liquid aluminium reacts with the carbon forming aluminium carbide. A shift in the metal pad height might in turn, expose the carbide to the electrolyte dissolving it. There can be aluminium droplets suspended in the molten salt due to turbulence. These can be oxidized at the anode in the presence of carbon dioxide resulting in alumina and carbon monoxide. Due to the design of the pot room the current induces a high electromagnetic field that results in interfacial stirring of the metal pad. Good compensation of the magnetic field has the effect of a stable metal pad and therefore increased current efficiency. The sodium level in the final product is however, high [17]. During anode change or tapping, there may result an electrical short circuit. This takes place when the carbon anode comes in direct contact with the liquid cathode. The physical losses that take place due to spillage while tapping are usually very small.

The most common and reliable way is to express it as the ratio between the produced mass of aluminium per unit of time and the theoretical mass calculated from Faraday's law:

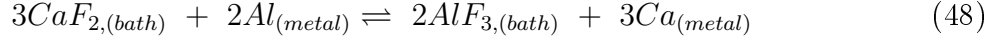
$$m_{theory} = \frac{ItM}{nF} \quad (47)$$

where I is the current in amperes, t is the duration of the electrolysis in seconds, M the molar mass of the metal produced, F is Faraday's constant (96485 C/mol) and n the number of electrons transferred. The main cathodic reaction is believed to be diffusion controlled. As a result the rate determining step is localized at the cathodic boundary layer and is mass transport controlled. The loss in cathodic current density is then a function of the electrolyte composition, temperature, mass transfer coefficients and overvoltage.

## 4.4 Impurities

Impurities in the production of aluminium can be metallic and non-metallic. Their presence can be traced back to the raw materials that are used to make up the electrolyte, the alumina feeding and the carbon anodes with additional impurities due to cell lining and tools used in the potroom [22]. It is therefore possible to further categorize the impurities as metal oxides with higher decomposition potential than alumina, metal oxides with lower decomposition potential than alumina, non-metallic oxides, sulphurous compounds and water.

The alkaline and alkaline earth metal oxides have higher decomposition than alumina and should therefore not co-deposit at the cathode. Among the most common ones are salts containing the ions:  $Na^+$ ,  $Ca^{2+}$ , and  $Mg^{2+}$ . NaOH is used in the extraction of bauxite therefore resulting in a considerable concentration of sodium in the alumina. However due to the equilibrium between the metal and electrolyte some alkaline metals will find their way into the metal produced [51]:



The losses in current efficiency due to impurities involve their partial reduction and oxidation, this being particularly true for polyvalent impurity species. According to Sterten et al. [23] the processes taking place at the cathode may be grouped in three steps, assuming that there are no concentration gradients within the bulk of the electrolyte:

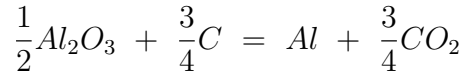
a) Mass transport of  $AlF_3$  to the cathode interface.

b) The main overall electrode reaction



c) Mass transport of  $NaF$  away from the cathode interface

Cathodic concentration overvoltages appear due to the rate limiting steps which are mass transport of  $AlF_3$  and  $NaF$  in the cathodic boundary layer. Therefore assuming a charge of  $3e^-$  the main overall cell reaction can be written as:



Some of the losses can be associated with impurities in the electrolyte forming dissolved metal species known as reduced entities or RE. The concentration of RE at the metal surface is much higher than in the bulk phase. As a result there are polyvalent impurity species taking part in cyclic redox reactions at the cathodic and anodic boundary layers. As Sterten et al [23] state the most important rate determining steps involved in the cyclic processes are:

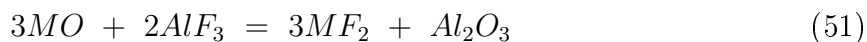
- i) mass transport of RE from the metal surface to a reaction plane within the cathode boundary layer
- ii) mass transport of impurity species from the electrolyte bulk phase to the reaction plane in the cathodic boundary layer.

The impurity enters the bath in its highest oxidation state (e.g.  $Ti^4$ ) and it dissolves in the bulk of the electrolyte. Convection transports the given element to the bulk/cathodic boundary layer where it is reduced by a RE to a lower oxidation state (e.g.  $Ti^3$ ). In the next phase the impurity can be further reduced by another RE to its elementary state and end up depositing at the cathode. Another mechanism involves the diffusion of the reduced specie back to the bulk of the electrolyte and transported, by convection, back up to the bath/anode gas interface where it can be reoxidized by  $CO_2$  back to a higher oxidation state.

As mentioned above the second type of impurities are non-metallic. By making the assumption that most of the impurities that are present in the bath are in the form of oxides or oxyfluorides the dissolution process could be described according to [22]:

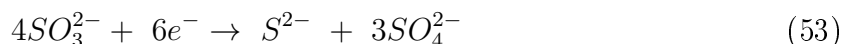
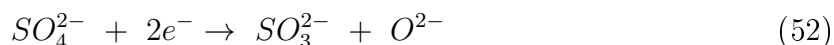


The impurities with a lower decomposition potential than the alumina have a tendency to be reduced at the cathode and end up in the metal produced. The others with a higher decomposition potential have the predilection of accumulating in the melt. The impurity of interest here is phosphorus. It can have several valence states from -3 to +5 and therefore plays an important role in reducing the current efficiency due to cyclic oxidation and reduction reactions[22]. The dissolution reaction involving a divalent cation will have the following form:

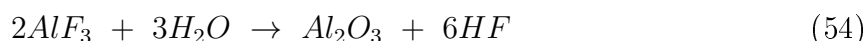


Due to the use of dry scrubbers, anode gases are recycled and therefore impurities find their way into the secondary alumina. As a result phosphorus and other impurities re-enter the electrolyte and could end up in the produced metal. The next section deals only with phosphorus since it is the main focus of this thesis.

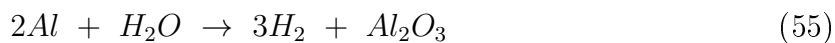
As mentioned above the rest of the impurities can be classified as sulphurous compounds and water. Sulphur is present in the petroleum coke at levels up to 3.5 wt% [46]. It combines with oxygen and leaves the cell as off-gas ( $SO_2$ ) but it can form COS,  $CS_2$  and  $H_2S$  as well. The chemical reduction of sulphate ( $S^{6-} - SO_4^{2-}$ ) anion by carbon and metallic aluminium results in the formation of sulphides and polysulphides ( $S^{-II}$ ) [45]. The electrochemical reduction of sulphate was found to take place according to the following equation which undergoes further chemical decomposition to sulphide and sulphate:



Water is yet another impurity that enters the process. It enters as atmospheric moisture either directly into the cell or adsorbed by raw materials such as alumina. The result is the hydrolysis of fluorides in the melt or the gas phase according to:



HF has been a great concern regarding the environment since it has a damaging effect. The dry scrubbers however are used to recycle the fluoride and send it back to the pots. Another detrimental factor concerning water is that it can react with aluminium metal according to:



The main concern here is that the free hydrogen dissolves in the metal and has a negative effect on the casting properties of the metal produced.

## 5 Phosphorus

### 5.1 General chemistry

Phosphorus was discovered by accident in 1669 by alchemist Hening Brand. He was searching for the mythical philosopher's stone and experimented with different materials. Among others he took a sample of urine which he distilled twice and calcined for a prolonged time resulting in a white glowing substance. The alchemist believed to have found elementary fire when in fact he obtained phosphorus[35].

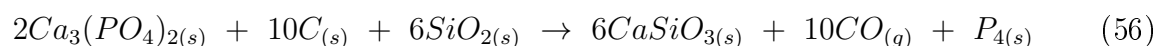
Phosphorus is one of the most abundant elements found on Earth with an average concentration of about 0.1% by weight. It is mainly used as fertilizer and is non-substitutable, being essential to life. Phosphorus has a wide range of applications but 80% of its production goes into fertilizers. The rest is used in the production of soaps and detergents, animal feed, food and medicine, electroplating and polishing of metals, military and more.

Phosphorus has a wide range of oxidation states from -3 to +5[36] and forms relatively stable bonds with many other elements. In the lithosphere phosphorus is found as a phosphate ion namely  $[\text{PO}_4]^{3-}$  in the pentavalence state. There is a wide variety of natural phosphates since phosphorus tends to form independent minerals even when it is in low concentrations[34]. Since phosphorus has a high affinity to oxygen it is not found in elemental state in nature. The most common phosphorus mineral is the phosphate rock which can be fluorapatite,  $\text{Ca}_5(\text{PO}_4)_3\text{F}$ , or calcium phosphate,  $\text{Ca}_3(\text{PO}_4)_2$ .

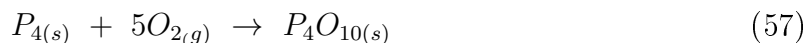


Figure 13: a) Fluorapatite mineral [29] b) Calcium phosphate rock [30]

In order to produce elemental phosphorus heating the calcium phosphate mineral with coke and silica sand is required:



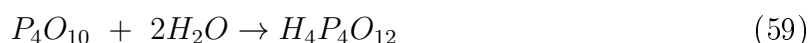
The most common allotropes of phosphorus are the white and red phosphorus. The white phosphorus has very high reactivity to oxygen, spontaneously bursting into flames when it comes in contact with air and therefore it is stored in water, in which, it is insoluble. The high reactivity to oxygen comes from its molecular structure which is a tetrahedron but with a bond angle of  $60^\circ$  instead of the usual  $109.5^\circ$ . In excess of oxygen an almost theoretical yield can be obtained from the reaction:



This oxide can appear in three forms. The first one, namely "H-form", is obtained by purification by sublimation in an oxygen atmosphere. When rapidly heated, this molecular compound, melts at a temperature of about 700 K and has a high affinity to water forming monophosphoric acid:



The above reaction takes place at room temperature or above, making phosphorus pentoxide a very effective dehydration agent. Under controlled conditions when the temperature is held below 280 K cyclotetraphosphoric acid can be formed:



The other 2 forms of the phosphorus pentoxide are formed by heating it at a temperature of 673 K in a closed vessel for 2 hours (O-form) and at the temperature of 723 K for 1 day respectively (O'-form). They have higher melting points namely 835 K and 853 K. The difference is that the "O-form" is a stable phase and dissolves slowly in water while the "O'-form" is a metastable phase and dissolves even slower in water. Neither is a molecular compound as the "H-form"[41].

Red phosphorus can be obtained by heating the white phosphorus at a temperature of about  $400^\circ\text{C}$  for several hours. Red phosphorus is less toxic than white, is less reactive to oxygen and can therefore be stored in air. The stability is given by the chain structure of the molecules.

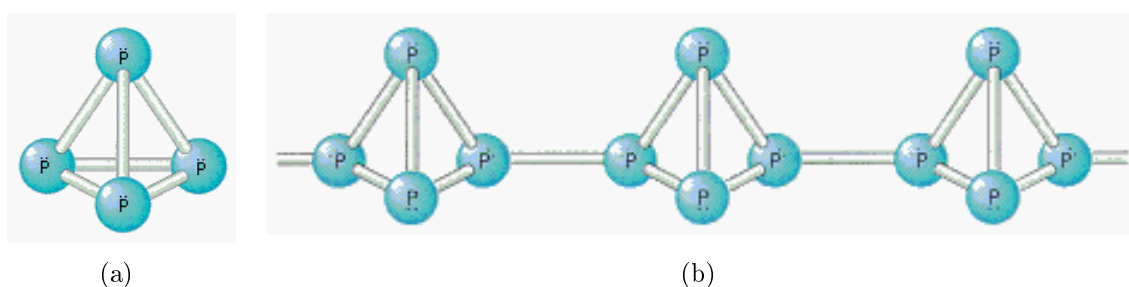
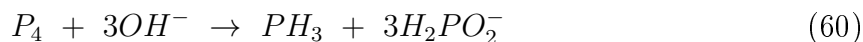
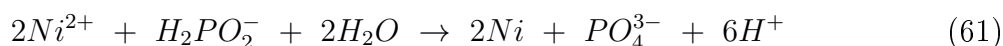


Figure 14: a) White phosphorus: tetrahedron structure. b) Red phosphorus: chain structure [37]

Phosphorus is found in group 5A in the periodic table with oxidation states being between -3 and +5. The most stable oxidation states are -3, 0, 1, 3 and 5. There are three most important oxyanions containing phosphorus all representing different oxidation states. The first one is hypophosphite where phosphorus is in oxidation state 1. It is formed in an alkaline solution where white phosphorus disproportionates according to:



Hypophosphine has a strong reducing effect and is thus used for nickel plating where  $H_2PO_3^-$  is used as the reducing agent and is oxidized to phosphite  $HPO_3^{2-}$  ( $P^3$ ) and then to phosphate  $PO_4^{3-}$  ( $P^5$ ). The main reaction can be written as:



The second stable oxidation state is 3 where all compounds are reducing agents and can be produced by partial oxidation of elementary phosphorus to form  $P_4O_6$  or  $P_4O_{10}$ . By reacting with water it would form  $H_3PO_4$  which is phosphoric acid. This can then form many salts containing the anions  $PO_4^{3-}$  (orthophosphate),  $PO_3^-$  (metaphosphate),  $HPO_4^{2-}$  hydrogenphosphate and  $H_2PO_4^-$  dihydrogenphosphate. The Lewis structures of the three most common anions are shown below:

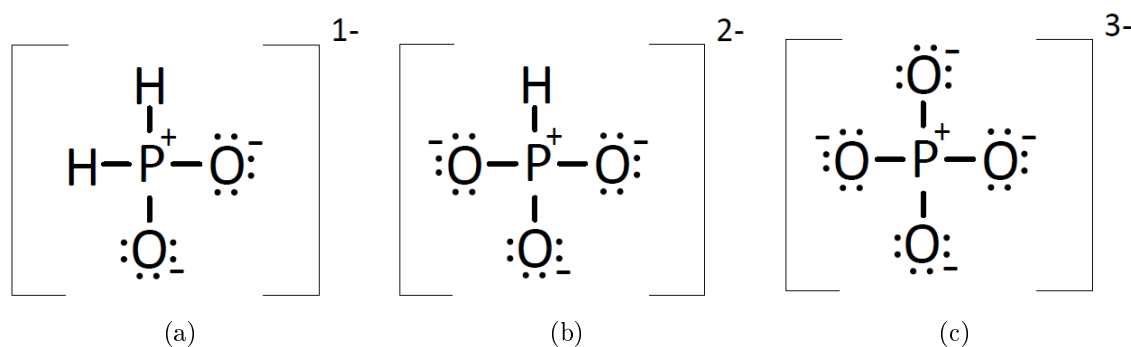


Figure 15: a) ( $P^1$ )  $H_2PO_2^-$  Hypophosphite. b) ( $P^3$ )  $HPO_3^{2-}$  Phosphite. c) ( $P^5$ )  $PO_4^{3-}$  Phosphate

Phosphorus has a melting point of  $44.3^\circ\text{C}$  and a boiling point of  $280.5^\circ\text{C}$ . The gaseous form contains molecules of  $P_4$  which can dissociate further as the temperature rises into:



The phosphorus will dissociate by 1% into  $P_2$  molecules at the temperature of  $800^\circ\text{C}$ . At the temperature of  $1200^\circ\text{C}$  about 50% of the  $P_4$  molecules would have converted into  $P_2$  and at temperatures above  $2000^\circ\text{C}$  further dissociation would reduce the molecules to free atoms.

The temperature of aluminium electrolysis is usually around  $950^\circ\text{C}$  and therefore elemental phosphorus would be present in its  $P_4$  and  $P_2$  molecular form.

Reaction (57) occurs even at room temperature. When the amount of oxygen is limited the following reaction will take place:



The adjustment of the oxygen pressure while heating elemental phosphorus would yield lower oxides, for example,  $P_2O_3$ .

In the industrial process, phosphorus enters the cryolite melt with the alumina and therefore most likely in the form of an oxide or phosphate. Analysis of the phosphorus content of alumina have been made by Danek et al. [39]. The phosphorus is presented as  $P_2O_5$ . Due to the humidity of air its strong affinity to water is more likely, however, that the phosphorus is present as aluminium phosphate or in hydrated form,  $H_3PO_4$ . Since the present experiments were limited to a laboratory cell aluminium phosphate was used,  $AlPO_4$ .

Experiments were performed by Thisted et al. [40] in order to determine the solubility of  $AlPO_4$  and to determine the phase diagram of the  $Na_3AlF_6 - AlPO_4$  system.

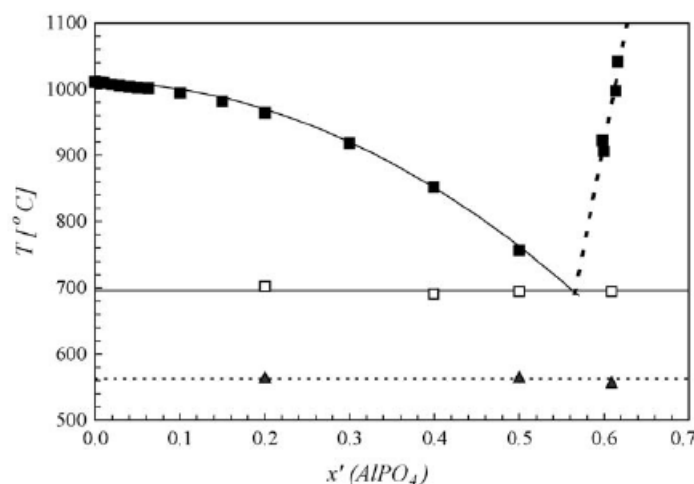


Figure 16: The phase diagram of the  $Na_3AlF_6 - AlPO_4$  determined through thermal analysis by Thisted et al. [40]

The phase diagram was determined to be a binary eutectic with the eutectic point being at 57.2mol% $AlPO_4$  at a temperature of 695.9°C.

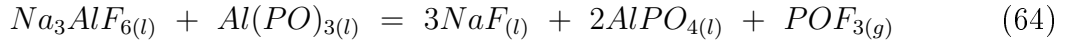
## 5.2 Impurity distribution in the aluminium electrolysis cell

Under normal conditions the concentration of phosphorus in the electrolyte may attain concentrations of up to 250 ppm thereby affecting the current efficiency. According to the literature each 100 ppm increase in phosphorus results in a decrease of approximately 1% in current efficiency. Danek et. al [39] performed a statistical analysis of the data collected from march to November 1997 from Slovalco, Slovakia. The phosphorus concentration was analyzed in primary and secondary alumina, aluminium fluoride, fresh and crushed electrolyte as well as carbon materials such as coke, pitch, prebakes and recycled anodes. The data collected is summarised in the table below.

Material	Concentration
Primary Al <sub>2</sub> O <sub>3</sub>	8.6 ± 1.3 ppm P <sub>2</sub> O <sub>5</sub>
Secondary Al <sub>2</sub> O <sub>3</sub>	75 ± 18 ppm P <sub>2</sub> O <sub>5</sub>
AlF <sub>3</sub>	209 ± 21 ppm P <sub>2</sub> O <sub>5</sub>
Fresh electrolyte	90 ± 43 ppm P <sub>2</sub> O <sub>5</sub>
Crushed electrolyte	215 ± 44 ppm P <sub>2</sub> O <sub>5</sub>
Al	3.5 ± 0.7 ppm P
Coke	2.1 ± 0.8 ppm P
Pitch	3.2 ± 1 ppm P
Recycled anodes	2.8 ± 0.6 ppm P

Table 3: Phosphorus concentration in different sources [39]

Studies were performed on the following reaction with cryolite:



The mixture was quenched and the weight loss was assumed to be due to the evaporation of POF<sub>(g)</sub>. The experimental values obtained for the weight loss were found to match the theoretical values calculated according to the reaction above.

Mol %	Weight loss (%)	Theoretical loss (%)	Compounds present
10	5.23	4.83	Na <sub>3</sub> AlF <sub>6</sub> , NaF
30	11.59	12.38	Na <sub>3</sub> AlF <sub>6</sub> , NaF, AlPO <sub>4</sub>
50	22.68	21.94	AlPO <sub>4</sub>
30	±	±	Amorphous
30	±	±	Na <sub>3</sub> PO <sub>4</sub> , aluminates Na <sub>2</sub> Al <sub>2</sub> O <sub>4</sub>

Table 4: The system given by Na<sub>3</sub>AlF<sub>6(l)</sub> + Al(PO)<sub>3(l)</sub> [39]

At the molar concentration of 10% the intensities of NaF were found to peak as in pure cryolite. When the molar concentration was raised to 30% it was observed that there was half of the Na<sub>3</sub>AlF<sub>6</sub> present than in the previous sample and traces of other compounds were noticed which were assumed to be AlPO<sub>4</sub>. As the concentration was increased even further to 50%, it was seen that the Na<sub>3</sub>AlF<sub>6</sub> was not present any more and that the remainder was glassy, the only compound being AlPO<sub>4</sub>.

In another study performed by Z. Qiu et al., the reduction of seven impurities in molten cryolite was observed. The impurities of interest were Fe, Si, P, Ti, V, Ni and Ga. The impurities were added to the bath and the contents analysed after four hours of thermal reduction and four hours of electrolysis under the same conditions. The level of the impurities was varied as well, from A to 2A, 4A and 8A. At the end of the experiment analysis was carried out on both bath and metal samples, thus determining the impurity

distribution. A ratio between the impurity content in the bath and impurity content in metal was taken which was named the equilibrium distribution coefficient.

$$K = \frac{\text{impurity content in bath (ppm)}}{\text{impurity content in metal (ppm)}} \quad (65)$$

The results showed that phosphorus has the highest coefficient of the studied impurities for both the chemical and electrochemical reduction with values being between 0.8 and 1.0. As a comparison the K values for the elements Fe, Ti, V, Ni and Ga were found to be less than 0.2 for thermal reduction and only between 0.01 and 0.02 in the case of electrolysis. Furthermore it was observed that the cathodic current density did not have any significant influence on the equilibrium coefficient.

The effects resulting from the installation of dry scrubbers in aluminium smelters was studied by Augood [32]. A relation between the distribution coefficients where bulk gas, metal and feed streams are in constant ratio. The gas/metal ratio, K, for phosphorus was assumed to be 10. The ratio between gas and feed of the cell is related to K by:

$$\alpha = \frac{K}{1 + K} \quad (66)$$

Since it was assumed that the K ratio is 10 for phosphorus,  $\alpha$  was calculated to 0.91 which was found to be confirmed by earlier data [32, 50].

### 5.3 The effects of phosphorus in the aluminium cell

Phosphorus is known to have two major detrimental effects in the electrolysis of aluminium. On the one hand it reduces the current efficiency and on the other hand phosphorus contamination of the produced aluminium lowers corrosion resistance and increases its brittleness.

The alloys most affected by the presence of phosphorus in aluminium are the hypo-eutectic primary foundry alloys (PFA) namely Al-Si alloys which are used for the production of cars engines. By looking at the phase diagram shown below it can be seen that the eutectic composition is at 12.6 wt% Si which has a melting point of 577° C.

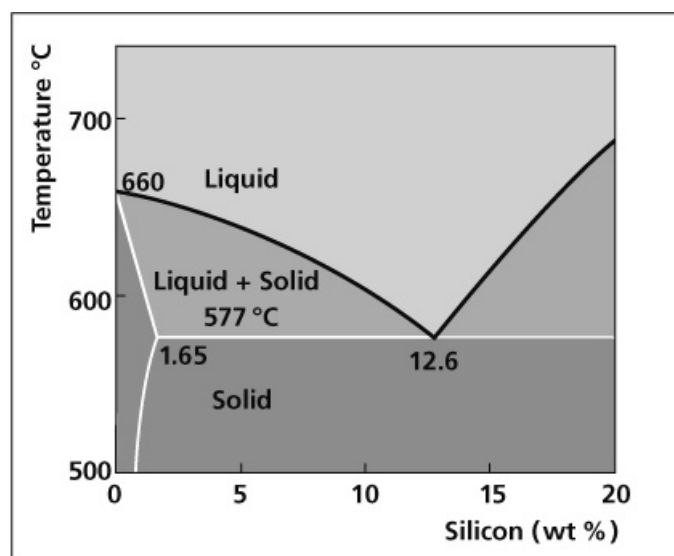


Figure 17: The phase diagram of the Al-Si [48]

The hypoeutectic alloys contain less than 12.6 wt% Si and are formed of an aluminium matrix in which small eutectic crystals of Al-Si are dispersed. The lower the size of the crystals the higher strength and ductility of the alloy is achieved. The eutectic temperature is lowered with additions of Na or Sr. The negative effect of P is due to nucleation sites formed around it in the molten metal for Al-Si eutectic crystals [55]. The effect can be suppressed by adding a higher amount of Na or Sr but a low phosphorus concentration is needed (lower than 10ppm).

According to Haugland et al. [22], these impurities are present in the electrolyte as dissolved fluoride or oxyfluoride complexes. As mentioned earlier the dissolution of a divalent cation will have the following form:



The impurities with a lower decomposition potential than the alumina have a tendency to be reduced at the cathode and end up in the metal produced. The others, with a higher decomposition potential, will have the predilection of accumulating in the melt. The impurity of interest here is phosphorus. It can have several valence states from -3 to +5 and therefore plays an important role in reducing the current efficiency due to cyclic oxidation and reduction reactions. Due to the use of dry scrubbers, anode gases are recycled and impurities accumulate in the secondary alumina. As a result there is a considerable amount of phosphorus that builds up in the electrolyte and ends up in the produced metal.

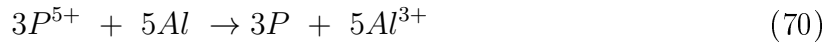
Phosphorus enters the melt along with the primary alumina in the form of an oxide or a phosphate. Usually the level is 0.001–0.002wt%P but this level can increase significantly due to the dry scrubbers. At concentrations of phosphorus lower than 1200 ppm a 2 electron cyclic redox reaction was proposed by Deininger and Gerlach [52] in order to explain the loss in current efficiency:



At concentrations higher than 1200 ppm the dominant equation becomes a 5 electron cycling reaction:



Another reaction that describes the behaviour of phosphorus in the presence of aluminium is shown below[42]:



However the above reaction does not provide an explanation for the loss in current efficiency. What can explain it, however, is that phosphorus is oxidized at the anode and reduced at the cathode in repeating cycles resulting in a prolonged lifetime within the melt. At the cathode the phosphorus species are reduced to gaseous elemental phosphorus. Due to its strong tendency to escape, little phosphorus would end up in the produced metal. The elemental phosphorus would then travel upwards towards the anode where it would be oxidized either by dissolved CO<sub>2</sub> in the melt or at the anode. Other dissolved P(V) species might be reduced by other impurities in the bath and carbon dust would act as nucleation sites. Phosphorus escapes the cell attached to carbon dust or by evaporation of gaseous elemental phosphorus which are later recycled with the secondary alumina [22].

Another mechanism involved is the condensation of the reduced phosphorus on the external crust over the melt which reoxidizes when coming in contact with oxygen in the

atmosphere. When the feeding of alumina takes place the crust is broken and thus the reoxidized phosphorus enters the bath once again[42].

## 5.4 Phosphorus circulation in the industrial process

In the early days of aluminium production the off gases were expelled straight into the atmosphere. However, environmental concerns due to fluoride emissions have provided the need for gas recycling systems.

Nowadays, the anode off gases are expelled from the cell and run through a dry scrubbing system. Alumina is used as the main component in the dry scrubbing systems since it has the ability to absorb fluoride and can be sent back to the cell. These have made possible the recovery of 98 – 99% of the fluoride thus minimizing the need for adding  $\text{AlF}_3$  to the melt which helps lower the liquidus temperature. On the other hand, impurities such as phosphorus may be recycled as well and sent back to the cell via the secondary alumina, rich in fluoride.

Attempts have been made at further developing the system so that the phosphorus and other impurities are not carried back to the electrolysis cell with the secondary alumina. High phosphorus level in the electrolyte results in cyclic redox reactions and therefore reduced current efficiency. Cutshall [42] has made a series of experiments trying to establish the method best suited for phosphorus cleaning of the secondary alumina. Thermal treatment at 400 – 1200° C showed no effect. Washing with sulphuric acid at 80° C removed 36% of the total phosphorus while sodium hydroxide washing at 50° C resulted in a 50% removal. An amount of 75% of P was removed by ultrasonic treatment of a water slurry with 25 wt% bulk secondary alumina. An even higher phosphorus percentage 80% was removed by means of flotation of a water slurry with 15 wt% bulk secondary alumina.

Another method was proposed by Schuh et. al [43] which involves a mechanical process for the removal of impurities from secondary alumina. The impurities are in the form of fines with sizes of less than 10 $\mu\text{m}$ . Due to the size some of them are attached to larger particles. Detachment is done by blowing the secondary alumina on a fixed impact plate, the particles being then separated by a cyclone and collected through filters. The impact-shock effect is a function of the impact velocity and the impact frequency. To ensure that fluorides or alumina are not part of the fines expelled the amount collected is kept at below 1% of the entire secondary alumina. Tests have shown that this percentage contains however 67% of the phosphorus and 49% of the iron in the scrubbing alumina.

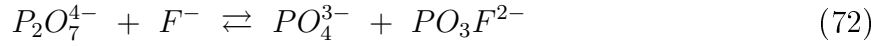
## 5.5 Electrochemistry of phosphorus

Phosphorus is an element that is known for its anions rather than cations. It can appear in salt-like phosphides ( $\text{PH}_3$ ), high molecular covalent phosphides (BP) and metallic phosphides ( $\text{M}_{>1}\text{P}$ , MP,  $\text{M}_{<1}\text{P}$ ). The ions can have the following forms:  $\text{P}^{3-}$ ,  $\text{P}_2^{4-}$ ,  $\text{P}_5^{3-}$ ,  $\text{P}_6^{4-}$ ,  $\text{P}_7^{3-}$ ,  $\text{P}_{11}^{3-}$ ,  $\text{P}_{21}^{3-}$ ,  $[\text{P}^-]_x$ ,  $[\text{P}_5^-]_x$ ,  $[\text{P}_7^-]_x$

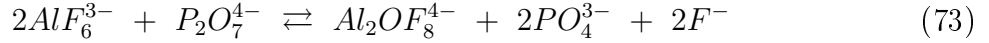
Bratland [47] conducted a study regarding the cryolite-sodium pyrophosphate melts where the dissociation of cryolite was assumed to be:



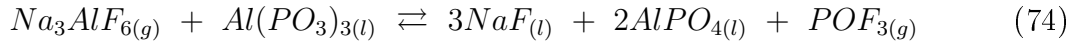
and the fluoride ions react further to form:



Another reaction proposed was:



When mixing cryolite with  $\text{Al}(\text{PO}_3)_3$  Danek et al. [39] found that the result was:



Experiments performed by Chrenkova et al. [49] with the systems  $\text{Na}_3\text{AlF}_6 - \text{Na}_3\text{PO}_4$ ,  $\text{Na}_3\text{AlF}_6 - \text{AlPO}_4$ , and  $\text{Na}_3\text{AlF}_6 - \text{Al}(\text{PO}_3)_3$  showed the formation of  $\text{PO}_4^{3-}$  from which it can be deduced that the orthophosphate ion is stable in molten cryolite.

Since phosphorus can have valencies varying from -3 to +5 it can form many compounds. Examples for each valency are given below:

Valence	Compound
-3	$\text{PH}_3$
-2	$\text{P}_2\text{H}_4$
-1	$(\text{PH})_n$
0	$\text{P}_4$
+1	$\text{H}_3\text{PO}_2$
+2	$\text{H}_4\text{P}_2\text{O}_4$
+3	$\text{H}_3\text{PO}_3$
+4	$\text{H}_4\text{P}_2\text{O}_6$
+5	$\text{H}_3\text{PO}_4$

Table 5: Examples of compounds containing phosphorus in different valence states.

In her doctoral thesis Thisted [50] conducted a thorough study of the data existing on phosphorus in an electrochemical context. Phosphorus species can be either oxidising or reducing agents depending on whether they appear in an acidic or basic solution. The Latimer diagrams for acidic and basic solutions of phosphorus are shown below, where the potentials, in Volts, are shown on the arrows and the valencies are given above the molecular formula. The temperature is set to 298K.

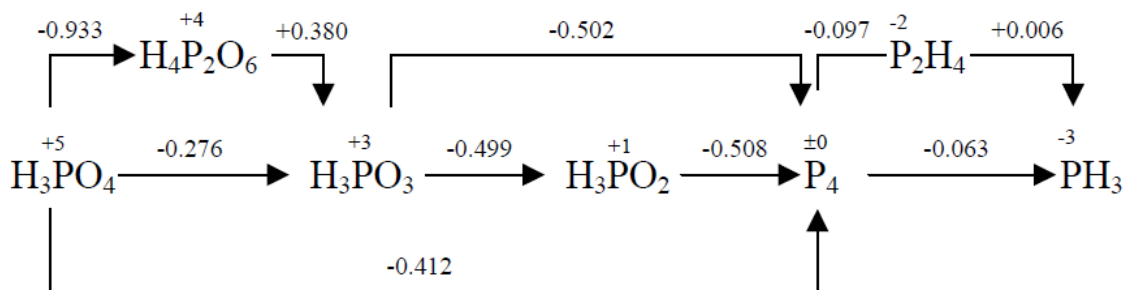


Figure 18: pH = 0 [50]

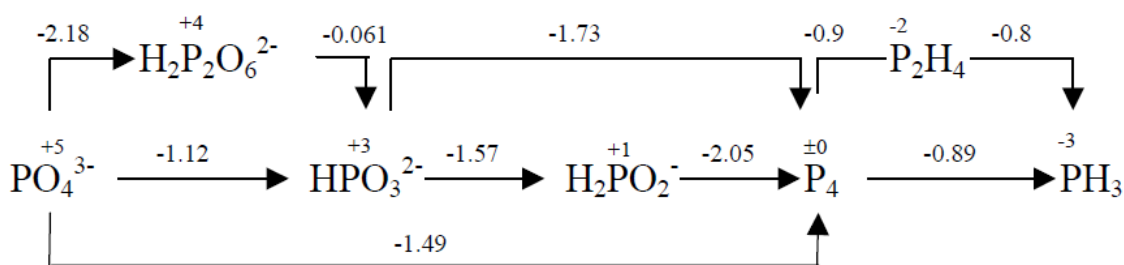


Figure 19: pH = 14 [50]

The electrochemical behaviour of phosphorus compounds in molten salts has not been thoroughly studied. In order to provide some comparison between the solutions (aqueous and molten salt), in their doctoral thesis both Thisted [50] and Keppert [51] use the electrochemical data from aqueous solutions against the aluminium reference electrode where  $E^\circ = -1.68$  V. The basic solution potentials with respect to SHE are used and shifted accordingly shown below:

Red-ox couple	Change in valence state	$E_{SHE}^{\circ}$ [V]	$E_{Al^{3+}/Al}^{\circ}$
$PO_4^{3-}/H_2P_2O_6^{-}$	5+ $\rightarrow$ 4+	-2.18	-0.50
$PO_4^{3-}/HPO_3^{2-}$	5+ $\rightarrow$ 3+	-1.12	0.56
$PO_4^{3-}/P_4$	5+ $\rightarrow$ 0	-1.49	0.19
$H_2P_2O_6^{-}/HPO_3^{2-}$	4+ $\rightarrow$ 3+	-0.061	1.62
$HPO_3^{2-}/H_2PO_3^{-}$	3+ $\rightarrow$ 1	-1.57	0.11
$HPO_3^{2-}/P_4$	3+ $\rightarrow$ 0	-1.73	-0.05
$H_2PO_3^{-}/P_4$	1 $\rightarrow$ 0	-2.05	-0.37
$P_4/P_2H_4$	0 $\rightarrow$ -2	-0.9	0.78
$P_4/PH_3$	0 $\rightarrow$ -3	-0.89	0.79
$P_2H_4/PH_3$	-2 $\rightarrow$ -3	-0.8	0.88

Table 6: Standard Potentials of the redox couples of phosphorus. The basic solution was taken as the starting point and the potentials expressed with respect to the standard hydrogen electrode (SHE) and the  $Al^{3+}/Al$  electrode.

However the difference in the solvents needs to be taken into account which means that these assumptions could be off. Further experimentation and investigation is needed for a better understanding of the electrochemistry of phosphorus in the molten salts. There are however studies done by Kerouantan [53] and Charlot et al. [54] focused on the behaviour of alkaline phosphates in molten cryolite at a temperature of  $1030^{\circ}C$ . Phosphorus was added as an alkaline orthophosphate and it was observed that a three valent species was obtained by a two electrons step reduction:



Additions of aluminium to the melt would reduce the five valent phosphorus to elementary P.

Deininger et al. [52] studied  $P_2O_5$  and its effects on current efficiency in the aluminium electrolysis. What they found was that when the phosphorus addition reached 0.12 wt% in the electrolyte its reaction behaviour changed. They suggested that the pentavalent phosphorus is reduced to trivalent phosphorus up to 0.12 wt%. Above the given concentration the phosphorus was reduced to its elemental state.

## 6 Experiments

### 6.1 Purpose of the experiments

In the aluminium industry the current efficiency is one of the most important parameters. Impurities play a detrimental role in the aluminium electrolysis either by being reduced at the cathode and ending up in the metal or, by taking part in cyclic redox reactions thus consuming electric current and reducing the current efficiency.

Phosphorus is one such impurity and a detailed study of the literature available was provided in the previous chapter of this work. Phosphorus can attain valence states between  $-3$  to  $+5$  it is oxidized at the anode and reduced at the cathode several times. These cyclic redox reactions are the reason for the prolonged residence time of phosphorus within the melt. It escapes the electrolysis cell attached to carbon dust or in gaseous elemental form [22].

Experiments were made in a laboratory cell to study the effects of phosphorus on the current efficiency. They were started on the premise that phosphorus forms volatile compounds and escapes the cell with the anode gases as shown in the work of Augood [32]. It was thus necessary to determine first the amount of phosphorus that escapes this particular electrolysis cell during the experiments in order to have a constant concentration throughout each experiment. Further work could then be performed involving different initial concentrations of phosphorus as well as current densities in order to determine the effects on current efficiency.

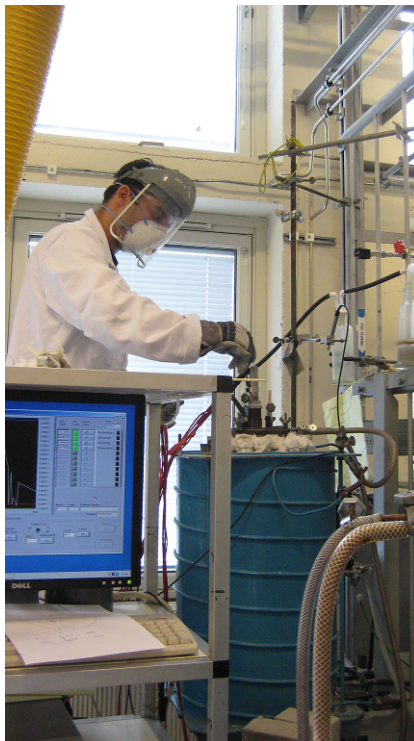


Figure 20: Petre Manolescu carrying out experiments at NTNU

## 6.2 Equipment setup

The experiments were carried out in a laboratory cell at the Sintef laboratory at the Norwegian Institute of Science and Technology. The furnace was designed and fabricated at Sintef since they are highly specialized and thus not found on the commercial market. The setup consisted of a small furnace connected to a power supply, with a water cooling system and inert gas cycle. The furnace is shown in the picture below:



Figure 21: The furnace and the main power supply.



Figure 22: The furnace viewed from the top side showing the Pythagoras tube and the anode tube within it before closing it up. The white wool was used as a heat insulator.

The furnace was open on both ends so that a Pythagoras tube could be fitted and closed with copper plates when in use. The lower lid had a metallic rod with radiation shields attached and a carbon support at the upper end. The crucible was then placed on top the carbon support and inside the Pythagoras tube. The carbon anode, 52 mm in diameter and 70 mm long, was screwed on top of a steel rod and placed inside the furnace with the rod protruding through the lid. The anode was designed with holes on the sides so as to allow the gases to escape. Furthermore, it had a  $10^\circ$  inward angled bottom in order to facilitate an upward movement of the gas bubbles. Needless to say the anode was changed after each experiment due to consumption and in order to prevent contamination of the bath from the previous experiment. The anode is shown in the figure below. The top lid was then connected to a water valve in order to keep it cool during the experiments. Failure to do so would result in overheating of the lid and damage to the soldering holding it together.

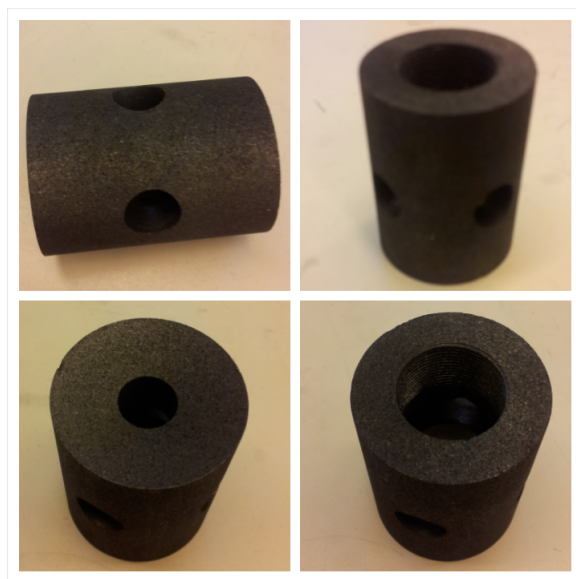


Figure 23: The carbon anode

Due to the high temperatures involved an inert gas atmosphere was required since carbon would burn in air. Nitrogen gas was used to ensure that the crucible would stay intact during the experiments with a flow rate of  $0.2 - 0.3 \text{ dm}^3/\text{min}$ . The furnace was connected to a power supply used for heating and maintaining temperature. A secondary DC power supply was used to supply the current during electrolysis. The negative pole was connected to the lower lid and the positive pole to the anode rod on the top of the furnace in order to attract the right charges during electrolysis. Rubber rings in an "O" shape were placed in creases within both the top and bottom lids. Grease was smeared on them to prevent air escaping through the locking of the copper plates with the ceramic tube. Rubber lids were provided for the anode tube since it was hollow.

After the furnace was turned on it was left for four hours to heat up and allow the melt to homogenize. The experiment itself took four hours with alumina feeding every fifteen minutes. Another 16 hours was needed to let the furnace cool off before opening it to retrieve the produced metal and make observations. Thus a total of twenty four hours were needed for each experiment.

Bath samples were taken during the experiment in order to analyse the phosphorus concentration. These were done at first with a carbon rod but later switched to a quartz tube in order to reduce the risk of contamination of the melt. These were taken at the beginning of the experiment, before the first feeding, during the experiment and one before switching the equipment off. Once the experiment was done everything was turned off except for the nitrogen gas and the cooling water. The furnace was opened, when cool, and the metal taken out by crushing of the crucible.

The furnace was cleaned properly after each experiment, refraining from the use of water since any moisture would be detrimental to the experiment. The top O rings needed changing after each use while the bottom ones could last for three to four experiments.

The cathodic support was changed every four experiments, its deterioration depending on the current density applied.

The Pythagoras tube was taken out after each run, cleaned and checked for cracks. If it showed signs of damage it had to be changed for the next experiment in order for it to be carried out properly.

The sintered alumina rod sheathing the thermocouple was inspected as well and changed if it showed signs of wear. It handled the heat well so there were no problems but it did break a few times since sintered alumina is hard but brittle.

### 6.3 Procedure

The cell setup consisted of a graphite crucible placed inside of a Pythagoras tube with nitrogen atmosphere. The carbon anode was designed to allow the anode gas bubbles to escape through the center. It had a vertical hole in the center to which a steel rod was attached. Furthermore there were two horizontal holes through it to allow movement of the electrolyte[25]. A steel pin, 4 mm in diameter and 20 mm long, was weighted and glued to the bottom of the crucible to provide conductivity.

A sintered aluminium lining of 65 mm in diameter and 110 mm in length was placed within the graphite crucible in order to protect it from the electrolyte. Another purpose it served was the prevention of alumina depletion within the bath and thus the anode effect. Alumina cement was then used as an insulator (8mm thick) around the pin and the crucible placed in a drying furnace at a temperature of about 200°C for 3 days. A schematic of the cell setup is shown in the figure below:

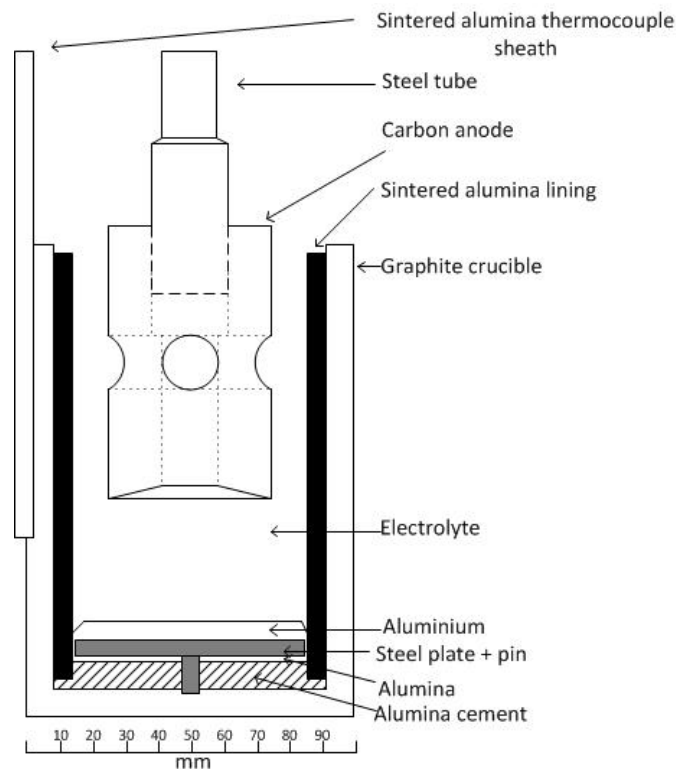


Figure 24: The cell

After the cement had dried alumina was placed on top of it. A steel plate with a diameter of 60 mm, a thickness of 5 mm and with a hole in the middle was weighted and placed on top of the alumina, through the pin, so that the plate and the pin were even. The steel plate was the wettable cathode giving a flat metal pad resulting in an even current distribution. The bath mixture was placed on top of the plate/pin plane and the crucible was kept in a drying furnace, while preparing the electrolysis furnace, to ensure there was no moisture left in the mixture. A side pocket on the crucible allowed the use of a thermocouple in order to keep track of the temperature of the cell. A Pt – PtRh10% thermocouple was placed in a sintered alumina tube and lowered inside the pocket of the crucible. This was then used to monitor the temperature of the melt throughout the experiments. In the first experiment a second thermocouple was used in order to establish the difference between the temperatures on the side of the crucible and inside.

The electrolyte contained the following composition, corresponding to a CR ratio ( $\text{NaF}/\text{AlF}_3$ ) of 2.5 with 4 wt%  $\text{Al}_2\text{O}_3$  and 5 wt%  $\text{CaF}_2$  :

1. Natural cryolite - 319 g
2.  $\text{Al}_2\text{O}_3$  - 15,13 g
3.  $\text{CaF}_2$  - 18,92 g
4.  $\text{AlF}_3$  - 25,2 g
5.  $\text{AlPO}_4$  - amount dependent on experiment

The amount of  $\text{AlPO}_4$  was varied between experiments since phosphorus was the impurity of interest in these experiments.

During electrolysis of alumina the impurities such as phosphorus tend to evaporate in time as anode gas. In order to be able to carry out the experiments properly the amount escaping the cell had to be determined experimentally. The current density was decided to be set at  $1.5 \text{ A/cm}^2$  which meant a DC current of 49.77 A.



Figure 25: The carbon crucible used, with the bath mixture already in place

After the bath had been mixed and dried, the crucible was placed on top of the cathodic support and inserted into the furnace from the bottom. The bottom end was closed with its proper lid including a well-greased "O-ring" that came in contact with the Pythagoras tube, thus sealing it. From the top side the thermocouple sheath was placed in the side-pocket of the crucible and then run through a hole in the lid along with the anode tube. A rubber cap was used for sealing the anode tube and a rubber hose was placed over the sintered alumina sheath of the thermocouple and tightened with a clamp. These measures prevented losses of anode gases to the environment. After sealing the furnace the nitrogen and water pump were turned on and the heating could begin. It was left to heat up for 4 hours in order for the melt to achieve the desired temperature of  $980^{\circ}$  and to homogenize properly.

The next step before starting the electrolysis was to connect the power supply to the anode and cathode and then find the contact point within the melt where it would start conducting current. There were two ways of finding this point. On the power supply there was the option of choosing between a set current or voltage. One way was to set the voltage to 2 V and lower the anode until there was current running between the anode and cathode. Another way was to set the current to 1 A and lower the anode until the current reached 1 A. Experimentally was found that the first method was easier. As soon as the contact point was found the anode was lowered by 19mm and fastened tight in that position. Although it was shown by Solli et. al. [25] that the interpolar distance in an experimental cell does not affect the current density unless there is direct contact between the anode gas bubbles and the cathodic boundary layer, a constant distance of 19 mm was maintained throughout the experiments.



Figure 26: Extraction of the metal formed was done by breaking the crucible. The interpolar distance was measured.

## 6.4 Experimental cases I - Results and discussion

As mentioned above, earlier work done by [32] suggests that phosphorus forms volatile compounds and escapes the cell with the anode gas. It was therefore necessary to establish the amount, if any, of phosphorus that escapes the cell during the experiments. The initial presumption was that phosphorus does leave the cell with the anode gas and was therefore decided to press tablets of phosphorus along with alumina and feed them manually through the anode tube. Bath samples were taken at regular intervals throughout the experiments. An inductive coupled plasma (ICP) analysis was performed on the samples in order to determine the concentration of phosphorus. The expectation was to observe a rather constant amount of the impurity in the samples taken. However the results showed a different trend as follows.

The first run was done with 600 ppm of phosphorus in the bath mix and a 10% addition of phosphorus with every feeding. This was done by pressing the phosphorus with 0.5 g of alumina powder into tablets and adding them to the melt. Another 3.45 g of alumina were fed each time giving a total of 3.95 g of alumina fed to the furnace every 15 minutes. Bath samples were taken just before the addition, in the beginning of the experiment, after about 2 hours and just before switching off the equipment. The equipment used was a carbon rod that was inserted through the anode tube and dipped slightly in the melt which would solidify on the cold rod and stay attached to it. A second method was imposed later in the experiments which was using a quartz tube which enabled sampling by suctioning bath into the tube. This was done in order to keep the samples from contamination since quartz is inert to the melt. The samples were then crushed into a fine powder and sent to a lab at St. Olav's hospital for ICP analysis. The analysis results showed the following:

Sample number	P concentration (ppm)
1	600
2	1057
3	1749

Table 7: ICP analysis results for experiment no. 1

The table above shows the results obtained from the ICP analysis. The samples were taken at three different times during the experiment. The first one was taken after fifteen minutes of electrolysis, just before the first feeding was to take place. The second sample was taken after about two hours, again, just before feeding. The last sample was taken just before the equipment was switched off and electrolysis ceased. Since the aim was to have a constant concentration of 600ppm throughout the experiment, the above results show clearly that the addition was too high. The concentration increases with each sample giving a final concentration of 1749 ppm. This suggests that the phosphorus added accumulated in the melt with little or nothing escaping.

For the next experiment the concentration addition was lowered to 6% of initial concentration. The same tablet addition procedure was carried out. The results are listed in the table below showing that yet again the addition percentage was too high, the final

concentration of phosphorus being 1569 ppm. The samples were taken at the same intervals as with the experiment before it. It was decided to lower the percentage addition once again for the third experiment.

Sample number	P concentration (ppm)
1	628
2	1062
3	1569

Table 8: ICP analysis results for experiment no. 2

The third experiment was carried out under the same conditions but with an addition of 5%. This time there were five samples taken: the first one just before the first addition and the rest at one hour intervals. The results are shown in the following table:

Sample number	P concentration (ppm)
1	546
2	880
3	1158
4	832
5	631

Table 9: ICP analysis results for experiment no. 3

Even though the final value is close to the initial one, there are fluctuations in the analysis results. This might suggest that the extra phosphorus added accumulated within the melt and managed to escape with the anode gases, or, that there was contamination between samples which could be due to the use of a carbon rod to extract the samples. A fourth experiment was carried out with no addition of phosphorus. Four samples were taken during the experiment. They were taken just before feeding after 15 minutes, 1.5 hours, 3 hours and lastly before switching the equipment off and ending the electrolysis. This time a quartz tube was used since it is inert to the melt and should provide higher purity of the samples. The following table shows the analysis results:

Sample number	P concentration (ppm)
1	614
2	597
3	601
4	651

Table 10: ICP analysis results for experiment no. 4

Table 6.4 shows that the concentration is rather stable. This implies that there is no phosphorus escaping from the cell over the duration of the experiment.

It has been established that under the above conditions phosphorus does not escape the electrolysis cell. That seems to contradict earlier results given by [32] but it was not meant as a test of that work. Given that the duration of the experiment is only 4 hours it might be that the volatile compounds do not have the necessary time to form. However the purpose of these experiments was to determine the conditions that are needed to maintain a stable concentration of phosphorus within the given cell. Having established that, future work will include changing the current density along with the initial concentration of phosphorus in the bath and observing their effects on the total current efficiency.

## 6.5 Experimental cases II - Results and discussion

Further experiments were performed with in collaboration with Rauan Meirbekova from University of Reykjavík as part of her doctoral thesis and are published in a paper at TMS 2014 [56]. These were performed in the same manner as the ones described above but varying the phosphorus concentration and the current density. The chosen current densities were 0.8 and 1.5 A/cm<sup>2</sup>. 13 experiments were carried out altogether with the phosphorus concentration varying from 0 to 600 ppm for current densities of 0.8 A/cm<sup>2</sup> and 1.5 A/cm<sup>2</sup>. There was some deviation, however, between the measured quantity of phosphorus added to the bath and the ICP analysis results of bath samples taken during the experiments. The results are shown in the following table.

Initial concentration [ppm]	ICP analysis [ppm]	Current density [A/cm <sup>2</sup> ]	Current efficiency [%]
0	N/A	0.8	93.53
0	N/A	0.8	93.03
0	N/A	1.5	94.97
50	39.3	0.8	93.16
50	41	1.5	94.7
100	80.6	0.8	92.96
100	79.1	1.5	93.35
254	223	0.8	91.24
254	230	1.5	90.06
254	211	1.5	89.76
600	412	0.8	89.89
600	634	0.8	89.46
600	506	1.5	90.9

Table 11: Comparison between different phosphorus concentrations and current densities and their effects on current efficiency

At the end of each experiment, after the furnace had cooled down, the crucible was taken out and broken. The metal was cleaned out and kept in an aqueous solution of  $\text{AlCl}_3 \cdot 6\text{H}_2\text{O}$  for 30 minutes. The metal extracted was cleaned and weighted after each experiment.

The current efficiency was measured by taking the ratio of the mass of aluminium formed during electrolysis and the theoretical mass as given by Faraday's law:

$$m_{Al} = \frac{ItM_{Al}}{nF} \quad (76)$$

where I is the current, t the time,  $M_{Al}$  the molar mass of aluminium, n the number of electrons transferred, in this case 3, and F Faraday's constant. The analyzed phosphorus concentrations were plotted against the current efficiency for the two different current densities.

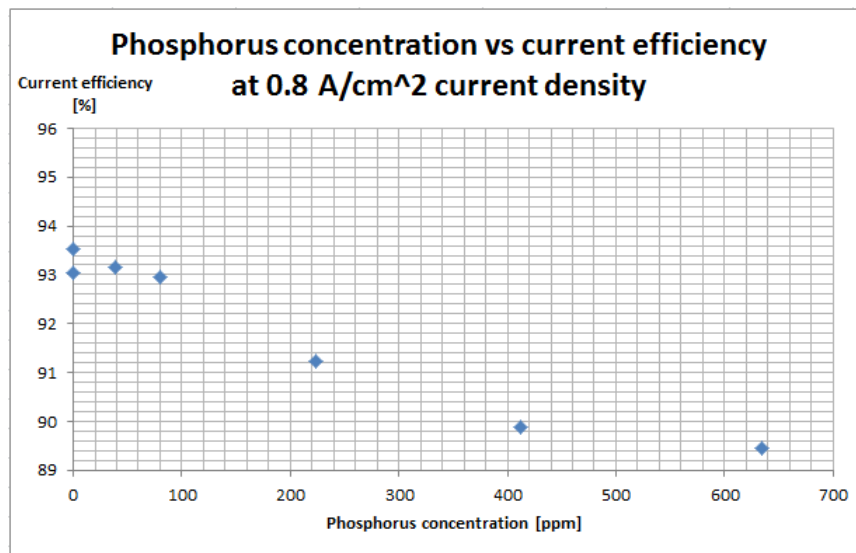


Figure 27: Phosphorus concentration vs. the current efficiency at 0.8A/cm² current density

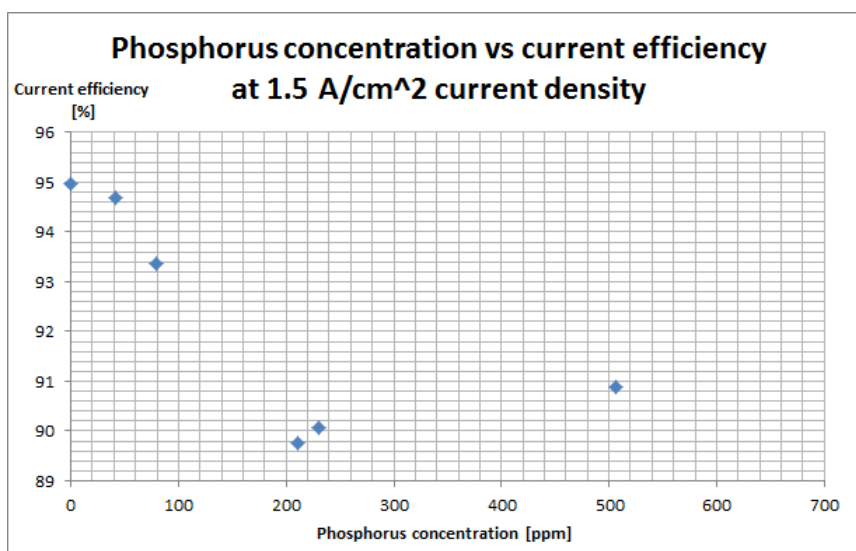


Figure 28: Phosphorus concentration vs. the current efficiency at 1.5A/cm² current density

These experiments show that increasing the phosphorus concentration decreases the current efficiency. For concentrations of up to 230 ppm of phosphorus the reduction in current efficiency is of about 2.4% per 100 ppm at a current density of 1.5 A/cm<sup>2</sup>. The CE reduction at 0.8 A/cm<sup>2</sup> was found to be 0.92%. Raising the current density to 1.8 and 2 A/cm<sup>2</sup> resulted in a lower current efficiency. These experiments were performed without addition of phosphorus in order to provide the benchmark measurements. The current efficiency was found to be 94.1% at 1.8 A/cm<sup>2</sup> and 93.8% at 2 A/cm<sup>2</sup> respectively. The current efficiencies in both cases were lower than the one for 1.5 A/cm<sup>2</sup> current density and no phosphorus addition, namely 94.97%. Therefore for this particular cell, the optimal current density lies below 1.8 A/cm<sup>2</sup>. An increase in the anode gas formation or stirring might take place within the cell at higher current densities and therefore affect the total current efficiency.

## 6.6 Conclusions and further work

Phosphorus is an impurity that is detrimental to the electrolysis of aluminium. Phosphorus has a long residence time in the electrolyte and takes part in a series of oxidation and reduction reactions. Since this was laboratory work, the raw materials were of high purity and therefore, the phosphorus was introduced as aluminium phosphate.

The premise was based on conclusions drawn from earlier work done by Augood [32] and Haugland et al. [22] which state that phosphorus escapes the cell with the anode gases. The ICP analysis performed on the bath samples prove that phosphorus does not escape the electrolysis cell. This seems to contradict the earlier work mentioned above but, it simply means that for the conditions under which these experiments were performed phosphorus remains within the melt. These conditions include the bath ratio, raw material purity, equipment used such as electrolysis cell and furnace along with sampling tools and duration of the experiments. Since they were run for only 4 hours it might be that the volatile compounds do not have the necessary time to form.

The experimental cases II show that the current efficiency decreases with increasing concentration of phosphorus within the melt. However the current efficiency depends on the current density as well. Measurements were performed while varying only one parameter at a time i.e. phosphorus concentration or current density. Experiments that were performed with a current density of 1.8 and 2 A/cm<sup>2</sup> were done with zero concentration of phosphorus to provide the benchmark measurements. Since they resulted in a lower current efficiency than at 1.5 A/cm<sup>2</sup> it is likely that there is an increase in gas evolution and thus fluid dynamic stirring that in turn affect the diffusion boundary layer. Another aspect is that this slight decrease in current efficiency could suggest that the cell itself has a maximum current efficiency point versus the current density due to its design and bath ratio used. Therefore, no other experiments were done at these high current densities. The effect of phosphorus in the reduction of current efficiency was found to be about 2.4% per 100 ppm at a current density of 1.5 A/cm<sup>2</sup>, for concentrations of up to 230 ppm of phosphorus. The CE reduction at 0.8 A/cm<sup>2</sup> was found to be 0.92% per 100ppm of phosphorus.

Further work could include the use of chemicals such as Na<sub>3</sub>PO<sub>4</sub> and Al(PO<sub>3</sub>)<sub>3</sub> as the source of phosphorus instead of AlPO<sub>4</sub>. The work of Danek et al. [39] deals with the possible reactions between cryolite and Al(PO<sub>3</sub>)<sub>3</sub> along with the phosphorus distribution between the aluminium, the melt and anode gases. However, it does not mention current efficiency. Experiments carried out in an industrial cell could be beneficial as well.

## References

- [1] Jomar Thonstad, Pavel Fellner, Geir Martin Haaberg, Ján Híves, Halvor Kvande, Åsmund Sterten. Aluminium Electrolysis Fundamentals of the Hall-Héroult Process. 3<sup>rd</sup> edition, Aluminium-Verlag Marketing & Kommunikation GmbH, 2001
- [2] Haupin Warren E., "Principles of Aluminium Electrolysis", Light Metals 1995
- [3] <http://herb-magic.com/alum-chunk.html>
- [4] Joseph W. Richards, "Aluminium - the metal of the future", The cosmopolitan magazine, 1892
- [5] <http://electrochem.cwru.edu/encycl/art-a01-al-prod.htm>
- [6] Solli P.A., Eggen T., Rolseth S., Skybakmoen E., Sterten Å., "Design and Performance of a Laboratory Cell for Determination of Current Efficiency in the Electrowinning of Aluminium", J. Appl. Electrochem., 26, 1019-1025(1996)
- [7] Sterten Å., Solli P. A., and Skybakmoen E., "Influence of Electrolyte Impurities on Current Efficiencies in Aluminium Electrolysis Cells", J. Appl. Electrochem., 28, 781-789(1998)
- [8] Sterten Å., "Redox Reactions and Current Loss in Aluminium Reduction Cells", Light Metals 1991, 445-451.
- [9] Hamann Carl H., Hamnett Andrew, Vielstich Wolf, "Electrochemistry", Second Completely Revised and Updated Edition, Weinheim: Wiley-VCH Verlag GmbH & Co. KGaA, 2007
- [10] Geir Martin Haaberg, lecture notes, NTNU, Spring 2013
- [11] Norman N. Greenwood, Alan Earnshaw, "Chemistry of the Elements", Second Edition, Butterworth-Heinemann, 1997
- [12] John Emsley, "Nature's building blocks and A-Z guide to the elements", Oxford University Press, 2001
- [13] Ian Polmear, "Light Alloys From Traditional Alloys to Nanocrystals", Fourth Edition, Elsevier Butterworth-Heinemann publications, 2006
- [14] K. Grjotheim, H. Kvande, "Introduction to Aluminium Electrolysis"
- [15] "Handbook of Aluminium, Volume 2, Alloy Production and Materials Manufacturing", edited by George E. Totten and D. Scott MacKenzie, Taylor & Francis e-Library, 2005
- [16] [http://www.csiro.au/news/newsletters/0702\\_metals/story3.htm](http://www.csiro.au/news/newsletters/0702_metals/story3.htm)
- [17] Tabereaux Alton T., "The role of Sodium in Aluminum Electrolysis: A Possible Indicator of Cell Performance", Light Metals, 1996
- [18] Ødegård R., Sterten Å., Thonstand J., Met. Trans., 19B, 444, 1988

- [19] <http://www.meritnation.com/ask-answer/question/draw-an-electrolytic-cell-and-label-the-following-a-anode-b-/chemical-effects-of-electric-current/3467267>
- [20] Jomar Thonstad, Elektrolyseprosesser
- [21] Richards Joseph W., "Aluminium - Metal of the future", 1892
- [22] Elin Haugland, Geir Martin Haaberg, Elke Thisted and Jomar Thonstad, "The Behaviour of Phosphorus Impurities in Aluminium Electrolysis Cells, Light Metals 2001
- [23] Sterten Å., Solli P. A., "Cathodic Processes and Cyclic Redox Reactions in Aluminium Electrolysis Cell", Journal of applied electrochemistry 1995, 25, pp 809-816
- [24] Sterten Å., "Redox Reactions and Current Loss in Aluminium Reduction Cells", Light Metals, 1991, pp. 445-451
- [25] Solli P. A., Haaberg T., Eggen T., Skybakmoen E., Sterten Å., "A Laboratory Study of Current Efficiency in Cryolitic Melts", Light Metals, 1994
- [26] Frode Seland "Electrochemistry", lecture notes, sept. 2012, NTNU.
- [27] <http://electrochem.cwru.edu/encycl/art-a01-al-prod.htm>
- [28] <http://www.epa.gov/aluminum-pfc/resources.html>
- [29] <http://hyperphysics.phy-astr.gsu.edu/hbase/minerals/fluorapatite.html>
- [30] [http://www.dep.state.fl.us/geology/geologictopics/rocks/hardrock\\_phosphate.htm](http://www.dep.state.fl.us/geology/geologictopics/rocks/hardrock_phosphate.htm)
- [31] S. Kolåsa, T. Størea, "Bath temperature and  $AlF_3$  control of an aluminum electrolysis cell, Control Engineering Practice, Vol 17, Issue 9, September 2009, pp. 1035-1043
- [32] D. R. Augood, "Impurities Distributions in Alumina Reduction Plants", Light Metals, 1980, pp 413-427
- [33] <http://hyperphysics.phy-astr.gsu.edu/hbase/tables/electpot.html>
- [34] Johan W. Brinck "World resources of phosphorus", A Ciba Foundation Symposium - Phosphorus in the Environment: its chemistry and biochemistry, Elsevier, 1978
- [35] D. N. Trifonov, V.D. Trifonov, "Chemical elements: how they were discovered", translation, Mir Publishers Moscow, 1985
- [36] R. J. P. Williams "Phosphorus biochemistry", A Ciba Foundation Symposium - Phosphorus in the Environment: its chemistry and biochemistry, Elsevier, 1978
- [37] R. Chang, K.A. Goldsby, "Chemistry", eleventh edition, McGraw-Hill international edition, 2013
- [38] D.D. Ebbing, S. D. Gammon "General Chemistry", eighth edition, Houghton Mifflin Company, 2005
- [39] V. Danek, M. Chrenkova, A. Silny, G. M. Haaberg, M. Stas, "Distribution of phosphorus in industrial aluminium cells", Canadian metallurgical quarterly, v. 38, pp 149-156, 1999

- [40] E. W. Thisted, G. M. Haarberg, J. Thonstad, "Solubility of  $\text{AlPO}_4$  in cryolite melts, *Thermochimica Acta* 447, pp 41-44, 2006
- [41] M. T. Averbuch, Pouchot A Durif, "Topics in phosphate chemistry", World Scientific Publishing, 1996 '
- [42] E. R. Cutshall, "Removal of phosphorus from dry scrubber alumina", *Light metals*, 1979
- [43] L. Schuh, G. Wedde, "Removal of impurities from dry scrubbed fluoride enriched alumina", *Light metals*, 1996
- [44] Z. Qiu, Y. Yu, M. He, X. Yu, B. Li, "Impurity distribution in bath and metal aluminium electrolysis", *Aluminium*, 75, 12, 1999, pp. 1110-1113
- [45] P. Fellner, M. Ambrová, J. Híves, M. Korenko, J. Thonstad, "Chemical and Electrochemical Reaction of Sulphur Species in Cryolite Melts, *Light Metals*, 2005, pp. 577-581
- [46] Seminary at Hydro Årdal, March 2013, as part of an NTNU field trip.
- [47] D. Bratland, H. Kvande, W. Q. Bin, "Ionic species in cryolite-sodium pyrophosphate melts", *Acta Chem. Scand.* A41, 1987, pp. 377-380.
- [48] <http://www.aluminium-brazing.com/2010/09/>
- [49] M. Chrenková, V. Daněk, A. Silný, "Reactions of phosphorus in molten cryolite", X. Slovak-Norwegian Symposium on Aluminium Smelting Technology, Stará Lesná-Ziar nad Hvom, Slovakia, Sep.21-23, 1999.
- [50] Elke W. Thisted, "Electrochemical properties of phosphorus compounds in fluoride melts", Doctoral thesis, NTNU, Trondheim, 2003.
- [51] Martin Keppert, "Electrochemical behaviour of phosphorus species in fluoride melts", Doctoral thesis, NTNU, Trondheim, 2006
- [52] L. Deininger, J. Gerlach, "Stromausbeutemessungen bei der Aluminiumoxid-Reduktionslektrolyse in Laboratoriumszellen", *Metall*, 33 2 pp 131-136, 1979
- [53] A. Kerounanton, "Comportement chimique et electrochimique de composés du phosphore dans la cryolithe fondue", *Revue de chimie minerale*, 1973
- [54] G. Charlot, J. Badozlambling, P. Homsy, V. Plichon, J. Saget, "Électrochimie des mélanges  $\text{NaF} + \text{AlF}_3$  fondus", 75, 2, 665-675, 1977
- [55] A. Knuutinen, K. Nogita, S.D. McDonald, A. K. Dahle, "Modification of Al-Si alloys with Ba, Ca, Y and Yb", *Journal of Light Metals*, Vol 1, Issue 4, 2001, pp 229-240
- [56] R. Meirbekova, J. Thonstad, G. M. Haaberg, G. Sævarsdóttir, "Effect of current density and phosphorus species on current efficiency in aluminium electrolysis at high current densities", TMS, 2014